

APPLIED SCIENCE ASSOCIATES INC APEX NC  
A STUDY OF TERRAIN SCATTERING PHYSICS. (U)  
AUG 80 G S BROWN

F/G 20/3

UNCLASSIFIED

RADC-TR-80-284

F19628-78-C-0211  
NL

146

END  
DATE  
FILMED  
4-2-80  
OTIC

54  
**RADC-TR-80-284**

**Interim Report**

**August 1980**

**LEVEL**



**A STUDY OF TERRAIN  
SCATTERING PHYSICS**

**Applied Science Associates, Inc.**

**Dr. Gary S. Brown**

AD A001520

**APPROVED FOR PUBLIC RELEASE; DISTRIBUTION UNLIMITED**

**DTIC  
ELECTE**  
NOV 3 1980  
S C

**DDC FILE COPY**

**ROME AIR DEVELOPMENT CENTER  
Air Force Systems Command  
Griffiss Air Force Base, New York 13441**

**8011 03 155**

This report has been reviewed by the RADC Public Affairs Office (PA) and is releasable to the National Technical Information Service (NTIS). At NTIS it will be releasable to the general public, including foreign nations.

RADC-TR-80-284 has been reviewed and is approved for publication.

APPROVED:

*Robert J. Papa*

ROBERT J. PAPA  
Project Engineer

APPROVED:

*William R. Baschnagel*

W.R. BASCHNAGEL, Lt Colonel, USAF  
Assistant Chief  
Electromagnetic Sciences Division

FOR THE COMMANDER:

*John P. Huss*

JOHN P. HUSS  
Acting Chief, Plans Office

**SUBJECT TO EXPORT CONTROL LAWS**

This document contains information for manufacturing or using munitions of war. Export of the information contained herein, or release to foreign nationals within the United States, without first obtaining an export license, is a violation of the International Traffic in Arms Regulations. Such violation is subject to a penalty of up to 2 years imprisonment and a fine of \$100,000 under 22 U.S.C 2778.

Include this notice with any reproduced portion of this document.

If your address has changed or if you wish to be removed from the RADC mailing list, or if the addressee is no longer employed by your organization, please notify RADC (EEC) Hanscom AFB MA 01731. This will assist us in maintaining a current mailing list.

Do not return this copy. Retain or destroy.

UNCLASSIFIED

SECURITY CLASSIFICATION OF THIS PAGE (When Data Entered)

REPORT DOCUMENTATION PAGE		READ INSTRUCTIONS BEFORE COMPLETING FORM
1. REPORT NUMBER (18) RADC-TR-80-284	2. GOVT ACCESSION NO. AD-A094	3. RECIPIENT'S CATALOG NUMBER 320
4. TITLE (and Subtitle) (6) A STUDY OF TERRAIN SCATTERING PHYSICS.	5. TYPE OF REPORT & PERIOD COVERED (9) Interim Report	6. PERFORMING ORG. REPORT NUMBER N/A
7. AUTHOR(s) (10) Dr. Gary S. Brown	8. CONTRACT OR GRANT NUMBER(s) (15) F19628-78-C-0211	9. PROGRAM ELEMENT, PROJECT, TASK AREA & WORK UNIT NUMBERS 61102F 2305J436 (17) J4L
10. PERFORMING ORGANIZATION NAME AND ADDRESS Applied Science Associates, Inc. 105 East Chatham Street Apex NC 27502 394248	11. CONTROLLING OFFICE NAME AND ADDRESS Deputy for Electronic Technology (RADC/EEC) Hanscom AFB MA 01731	12. REPORT DATE August 1980
13. MONITORING AGENCY NAME & ADDRESS (if different from Controlling Office) Same (11) Aug 80 (12) 7/6/	14. SECURITY CLASS. (of this report) UNCLASSIFIED	15. DECLASSIFICATION/DOWNGRADING SCHEDULE N/A
16. DISTRIBUTION STATEMENT (of this Report) Approved for public release; distribution unlimited		
17. DISTRIBUTION STATEMENT (of the abstract entered in Block 20, if different from Report) Same		
18. SUPPLEMENTARY NOTES RADC Project Engineer: Robert J. Papa (RADC/EEC)		
19. KEY WORDS (Continue on reverse side if necessary and identify by block number) Electromagnetic Scattering Rough Surface Scattering Radar Cross Section SIGMA DEC 78		
20. ABSTRACT (Continue on reverse side if necessary and identify by block number) This report presents interim results of a study to improve existing models for scattering from rough terrain. The two-scale composite surface model is first corrected to properly account for shadowing. This correction shows that both the optical and Bragg scattering terms in the expression for go to zero as grazing incidence is approached. The shadowing function for non-Gaussian surfaces is shown to be easily obtained from existing theories and numerical results for exponentially		

DD FORM 1 JAN 73 1473 EDITION OF 1 NOV 65 IS OBSOLETE

UNCLASSIFIED

SECURITY CLASSIFICATION OF THIS PAGE (When Data Entered)

394248

set

UNCLASSIFIED

SECURITY CLASSIFICATION OF THIS PAGE(When Data Entered)

distributed surfaces are presented. The two-scale composite surface based upon the Burrows perturbation theory is extended to the following cases; bistatic scattering from a dielectric surface with small scale roughness, and bistatic scattering from a dielectric surface with large and small scales of roughness. Comparisons are made with the Rice theory for both cases. Finally, it is shown how an existing theoretical relationship between the height and slope probability density functions can be used in practically obtaining one from the other.

Accession For	
NTIS GRA&I	<input checked="checked" type="checkbox"/>
DTIC TAB	<input type="checkbox"/>
Unannounced	<input type="checkbox"/>
Justification	
By _____	
Distribution/	
Availability Codes	
Dist	Avail and/or Special
A	

UNCLASSIFIED

SECURITY CLASSIFICATION OF THIS PAGE(When Data Entered)

# TABLE OF CONTENTS

	Page
1.0 INTRODUCTION. . . . .	1
1.1 Summary of Results . . . . .	2
2.0 A CORRECTION TO THE COMPOSITE SURFACE SCATTERING MODEL. . . . .	4
2.1 Background . . . . .	4
2.2 Discussion of the Error. . . . .	4
2.3 Correct Analysis . . . . .	7
2.4 Discussion of Numerical Example. . . . .	15
2.5 Summary. . . . .	18
References. . . . .	20
3.0 SHADOWING BY NON-GAUSSIAN RANDOM SURFACES . . . . .	21
3.1 Background . . . . .	21
3.2 Analysis . . . . .	21
3.3 Example. . . . .	27
3.4 Summary. . . . .	29
References. . . . .	31
4.0 BISTATIC SCATTERING FROM LOSSY RANDOM SURFACES. . . . .	32
4.1 Background . . . . .	32
4.2 Backscattering From A Dielectric Surface With Small Scale Roughness. . . . .	33
4.2.1 Horizontal Polarization . . . . .	37
4.2.2 Vertical Polarization . . . . .	40
4.3 Bistatic Scattering From A Dielectric Surface With Small Roughness. . . . .	44
4.3.1 Horizontal Polarization . . . . .	44
4.3.2 Vertical Polarization . . . . .	46
4.3.3 Cross Polarization. . . . .	49
4.4 Bistatic Scattering From A Dielectric Surface With Composite Roughness. . . . .	52
References. . . . .	63
5.0 A USEFUL RELATIONSHIP FOR THE JOINT SLOPE PROBABILITY DENSITY FUNCTION . . . . .	65

TABLE OF CONTENTS (Cont'd.)

	Page
5.1 Background . . . . .	65
5.2 The Transformation . . . . .	66
References. . . . .	69

## 1.0 INTRODUCTION

As radar systems designs become more complex and versatile, their performance becomes increasingly sensitive to the operational environment. This places an increased burden on the designer to incorporate the effects of the environment in system design studies. However, before this can be done, it is necessary to develop an accurate model of the environment. In the case of ground clutter or multipath, this means that there is a need for rough surface scattering models. Such models must not only be based upon sound physical principles but also exhibit agreement with measurements.

The purpose of this study is to provide improved models for surface scattering from terrain in the microwave frequency range and near grazing incidence. The basic approach entails applying the composite surface scattering theory to a lossy, randomly rough, dielectric surface. As long as the incident energy is not too near grazing and the surface is reasonably free of sharp edges or cusps, the composite model should be a reasonable description of the scattering process. Since the composite model is based upon the combining of two asymptotic scattering theories, it is approximate. Thus, an additional goal of this study is to investigate new techniques for improving the composite model. As our understanding of the scattering process increases and the models become more accurate, complex factors such as vegetation and snow cover can be studied, analyzed, and incorporated into the basic model. Thus, the overall effort comprises a phased approach.

This interim report details the initial results of the study. Present and future efforts on this investigation will be concerned with a more detailed study of some of the results reported here and also obtaining improved models for the coherent or average scattered field.

### 1.1 Summary of Results

Section 2 corrects an error in the basic composite scattering model. In particular, it is shown that shadowing is improperly accounted for and this error is corrected. In the corrected version of the composite model, it is shown that the conventional shadowing function multiplies both the zeroth and first order incoherent scattered power perturbation terms. Thus, even for a perfectly conducting surface the first order term will go to zero for back-scattering at grazing incidence due to the shadowing function. The first order perturbation power suffers an additional attenuation due to the shadowing of unfavorably oriented large scale surface slopes; however, this effect is relatively small compared to the impact of the conventional shadowing function.

Section 3 demonstrates how the shadowing function for non-Gaussian may be quite easily obtained from existing shadowing theories. The important surface characteristic in the general case is the probability density function of the large scale slopes in the plane of incidence. Explicit results are obtained for a surface characterized by roughness whose probability density function is exponential. The results of this study are particularly important for terrain scattering because terrain cannot always be described by a Gaussian height probability density function.

Section 4 extends the composite model to bistatic scattering from a lossy, dielectric, rough surface. The details are presented for three cases of increasing complexity; backscattering from a surface with only small scale roughness, bistatic scattering from a surface with only small scale roughness, and, finally, bistatic scattering from a composite (large and small scales of roughness) surface. This approach is a logical progression from the simple to the complex and is therefore beneficial to the reader. Furthermore, this

approach facilitates checking the results of the perturbation theory against existing solutions.

Section 5 discusses one technique for relating the joint probability density function of the surface heights to the joint density function for the slopes. The technique was originally obtained from an analysis of optical scattering from a rough surface but its relevance to this problem has apparently been overlooked. Although the technique is not always applicable to measured data, there are cases where it can provide the desired transformation.

## 2.0 A CORRECTION TO THE COMPOSITE SURFACE SCATTERING MODEL

### 2.1 Background

In [1], a solution to the problem of backscattering from a randomly rough, perfectly conducting surface comprising both large and small scales of roughness was presented. As a direct consequence of the stipulation that the surface roughness was a zero mean jointly Gaussian process, the scattering cross section per unit area was determined to be the sum of two terms, i.e.

$\sigma_{pp}^0(\theta, \phi) = [\sigma_{pp}^0(\theta, \phi)]_0 + [\sigma_{pp}^0(\theta, \phi)]_1$ . The  $[\sigma_{pp}^0(\theta, \phi)]_0$  contribution is dominant near normal incidence and results from the shadow corrected optical like reflection from properly oriented facets or specular points on the surface. The  $[\sigma_{pp}^0(\theta, \phi)]_1$  term is due to Bragg resonance scattering from the small scale surface features with appropriate accounting for the resonance broadening effects of the large scale surface undulations. Although shadowing is formally accounted for in a correct manner in the  $[\sigma_{pp}^0(\theta, \phi)]_1$  term, there is an error in the exact representation of the shadowing function which leads to an incorrect estimate of the effects of shadowing on large angle of incidence scattering. The goal of this section is to correct the above error and to properly account for the effect of large scale shadowing on the small scale scattering term.

### 2.2 Discussion of the Error

The analysis presented in [1] relating to the determination of  $[\sigma_{pp}^0(\theta, \phi)]_1$  is correct up to and including equation (23). The problem with the analysis following (23) is a result of inadequate attention to the definition of the shadowing function  $R(\theta, \phi)$ . That is,  $R(\theta, \phi)$ , as it appears in (23) of [1], can and should be expressed as follows;

$$R(\theta, \phi) = \overline{P^{(0)}} \left( \hat{k}_1 \mid \zeta_{lx} = \frac{k_{ox}}{B}, \zeta_{ly} = \frac{k_{oy}}{B} \right) \quad (2.1)$$

where

$$\overline{P^{(0)}}(\hat{k}_1 | \zeta_{lx}, \zeta_{ly}) = \langle P^{(0)}(\hat{k}_1 | \zeta_l, \zeta_{lx}, \zeta_{ly}) \rangle_{\zeta_l} \quad (2.2)$$

is the probability that an incident ray having direction  $\hat{k}_1$  will intersect a point on the large scale surface with orthogonal slopes  $\zeta_{lx}$  and  $\zeta_{ly}$  and will not be shadowed by any other part of the surface regardless of the height  $\zeta_l$  of the point in question. The symbol  $\langle \cdot \rangle_{\zeta_l}$  in (2.2) denotes the ensemble average over all values of large scale height  $\zeta_l$  and the notation  $P^{(0)}(\cdot)$  is the same as that employed by Sancer [2] in his excellent analysis of the effect of shadowing on  $[\sigma_{pp}^0, (\theta, \phi)]_0$ . It should be noted that as a result of the integrations in (23) of [1], the shadowing function  $R(\theta, \phi)$  is equal to  $\overline{P^{(0)}}(\cdot)$  evaluated at the specific large scale slope values given by  $\zeta_{lx} = k_{ox}/B$  and  $\zeta_{ly} = k_{oy}/B$  where  $k_{ox} = -2k_0 \sin \theta \cos \phi$ ,  $k_{oy} = -2k_0 \sin \theta \sin \phi$ ,  $B = 2k_0 \cos \theta$ ,  $\theta$  is the angle of incidence relative to the normal to the mean ( $\zeta=0$ ) plane, and  $\phi$  is the azimuth direction of incidence.

In order to more clearly understand and therefore rectify the error in [1], it is beneficial to repeat equation (23) of [1], i.e.

$$\begin{aligned} & \frac{1}{2\pi} \int_{-\infty}^{\infty} \int_{-\infty}^{\infty} \left\langle I(x_1, y_1) I(x_2, y_2) f_{pp}(\zeta_{lx_1}, \zeta_{lx_2}, \zeta_{ly_1}, \zeta_{ly_2}) \exp[jB(\zeta_{l_2} - \zeta_{l_1})] \right\rangle \\ & \cdot \exp(-jk_{ox}\Delta x - jk_{oy}\Delta y) d\Delta x d\Delta y \approx R(\theta, \phi) f_{pp}\left(\frac{k_{ox}}{B}, \frac{k_{ox}}{B}, \frac{k_{oy}}{B}, \frac{k_{oy}}{B}\right) \\ & \cdot \frac{1}{2\pi} \int_{-\infty}^{\infty} \int_{-\infty}^{\infty} \exp\left\{-j(k_{ox}\Delta x + k_{oy}\Delta y) - 4k_0^2 \cos^2 \theta \overline{\zeta_l^2} [1 - \rho_l(\Delta x, \Delta y)]\right\} d\Delta x d\Delta y \end{aligned} \quad (2.3)$$

where  $\Delta x = x_2 - x_1$  and  $\Delta y = y_2 - y_1$ . In (2.3)  $I\left(\frac{x_1}{2}, \frac{y_1}{2}\right)$  is one if the point  $\left(\frac{x_1}{2}, \frac{y_1}{2}, \zeta_{\ell 1}\right)$  on the large scale surface having slopes  $\zeta_{\ell x_1}$  and  $\zeta_{\ell y_1}$  is illuminated and zero if it is shadowed. The function  $f_{pp}$  is defined in [1],  $\overline{\zeta_{\ell}^2}$  is the mean square height of the large scale surface, and  $\rho_{\ell}(\cdot)$  is the normalized autocorrelation function of the large scale surface height. It should be noted that the left hand side of (2.3) represents the Fourier transform of the  $\langle \cdot \rangle$  term (from  $\Delta x \Delta y$ -space to  $k_{ox} k_{oy}$ -space) and (2.3) is supposed to show where the transform variables appear in the result. Such knowledge is essential to accomplishing the convolution of (2.3) with the small scale surface height spectrum because this convolution determines  $[\sigma_{pp}^0]_1$ . That is, in the convolution  $k_{ox}$  and  $k_{oy}$  must be replaced by  $k_{ox} - k_x$  and  $k_{oy} - k_y$  where  $k_x$  and  $k_y$  are the new variables of integration (see (32) of [1]).

If  $R(\theta, \phi)$  in (2.3) had been replaced by its precise definition, as given by (1), the problem of determining where  $k_{ox}$  and  $k_{oy}$  appear in the right hand side of (2.3) would have been correctly solved. Unfortunately, this was not done. Instead,  $R(\theta, \phi)$  was incorrectly written as  $(1 + C_0)^{-1}$  and, through the use of trigonometric manipulations,  $C_0$  was expressed in terms of  $k_{ox}$  and  $k_{oy}$ , see equations (24) through (28) in [1]. This development failed to recognize that  $C_0$  does not, in general, depend upon the transform variables in (2.3). That is, if one changes the transform variables from  $k_{ox}$  to  $k_x$  and from  $k_{oy}$  to  $k_y$ ,  $C_0$  would still only depend on  $k_{ox} = -2k_0 \sin \theta \cos \phi$  and  $k_{oy} = -2k_0 \sin \theta \sin \phi$ . The primary consequence of this error is to provide an incorrect formula for  $R(\cdot)$  for use in all equations following (28) in [1]. As will be shown, this error fortunately has negligible consequence on the numerical results presented in [1].

### 2.3 Correct Analysis

The error identified and explained above can be rectified by determining the functional dependence of the right hand side of (2.1) upon the large scale slopes  $\zeta_{lx}$  and  $\zeta_{ly}$  since they are replaced by the transform variables  $k_{ox}$  and  $k_{oy}$ . This can be done in a relatively straightforward manner by generalizing Smith's [3] results to the case where  $\hat{k}_1$  is at an angle  $\pi/2 - \phi$  with respect to the y-axis rather than directly along the y-axis. Such a generalization leads to the following;

$$\overline{P^{(0)}}(\hat{k}_1 | \zeta_{lx}, \zeta_{ly}) = \frac{U(\text{ctn } \theta - \zeta_{lx} \cos \phi - \zeta_{ly} \sin \phi)}{1 + C_0} \quad (2.4)$$

where  $C_0$  is given by (24) of [1] and  $U(\cdot)$  is the unit step function which is one if the argument is positive and zero if the argument is negative. Of particular note in (2.4) is the fact that  $\zeta_{lx}$  and  $\zeta_{ly}$  only appear in the argument of the unit step function. Substituting (2.4) into (2.1) yields the correct expression for  $R(\theta, \phi)$ , i.e.

$$R(\theta, \phi) = \frac{U(\text{ctn } \theta - \frac{k_{ox}}{B} \cos \phi - \frac{k_{oy}}{B} \sin \phi)}{1 + C_0} \quad (2.5)$$

If one substitutes  $k_{ox} = -2k_0 \sin \theta \cos \phi$  and  $k_{oy} = -2k_0 \sin \theta \sin \phi$  in (2.5) such as required in the determination of  $[\sigma_{pp}^0]_0$ , then  $R(\theta, \phi) = (1 + C_0)^{-1}$  and it will depend only on the angles  $\theta$  and  $\phi$  and the mean square slopes  $\overline{\zeta_{lx}^2}$  and  $\overline{\zeta_{ly}^2}$  of the large scale surface (see equations (24) and (25) of [1]). However, in the convolution expression for  $[\sigma_{pp}^0]_1$ , the unit step function must be retained. That is, one must use the following relationship;

$$R\left(\frac{k_{ox} - k_x}{2k_0 \cos \theta}, \frac{k_{oy} - k_y}{2k_0 \cos \theta}\right) = \frac{U\left(\text{ctn } \theta - \left[\frac{k_{ox} - k_x}{2k_0 \cos \theta}\right] \cos \phi - \left[\frac{k_{oy} - k_y}{2k_0 \cos \theta}\right] \sin \phi\right)}{1 + C_0} \quad (2.6)$$

Equation (2.6) leads to a completely different interpretation of the effects of large scale shadowing on  $[\sigma_{pp}^0]_1$  from that erroneously presented in [1]. According to (2.6), shadowing now gives rise to an attenuation factor  $(1+C_0)^{-1}$  which is common to both  $[\sigma_{pp}^0]_0$  and  $[\sigma_{pp}^0]_1$ . This result is merely a consequence of the fact that small areas on the surface capable of producing strong Bragg scatter, i.e.  $\zeta_{lx} = \zeta_{ly} = 0$ , are as equally shadowed as the areas properly oriented for specular reflection, i.e.  $\zeta_{lx} = k_{ox}/B$  and  $\zeta_{ly} = k_{oy}/B$ . This statement can be easily verified by noting that for both sets of the above values of  $\zeta_{lx}$  and  $\zeta_{ly}$ ,  $U(\text{ctn}\theta - \zeta_{lx} \cos \phi - \zeta_{ly} \sin \phi) = 1$  in equation (2.4) and so  $R(\theta, \phi) = (1+C_0)^{-1}$ . Since both the  $[\sigma_{pp}^0]_0$  and  $[\sigma_{pp}^0]_1$  terms suffer the same attenuation due to shadowing, the transition region in  $\theta$  (where  $[\sigma_{pp}^0]_0$  decreases and  $[\sigma_{pp}^0]_1$  becomes predominant) is independent of shadowing effects. Since shadowing results from the slopes of the large scale surface structure and since the large scale slopes are not the important surface characteristic in determining the transition region, this result demonstrates that the theory is self consistent.

The unit step function in (2.6) serves the very important purpose of establishing the limits on the integrals in the convolutional expression for  $[\sigma_{pp}^0]_1$ , see (32) of [1]. However, before this aspect of the problem is considered, it is worthwhile reviewing the physics behind the reason for the unit step function in (2.6). The unit step function appears in (2.6) because there is a certain range of surface slope values for which the probability of having an incident ray shadowed is identically one [3]. This result may be readily understood by referring to Figure 2.1. In (a), the slope of the surface is negative at the point of intersection and the incident ray is not shadowed in a small neighborhood of the point. In (b), the surface slope is equal to the slope of the incident ray ( $\text{ctn}\theta$ ) and the ray is therefore tangent to the surface

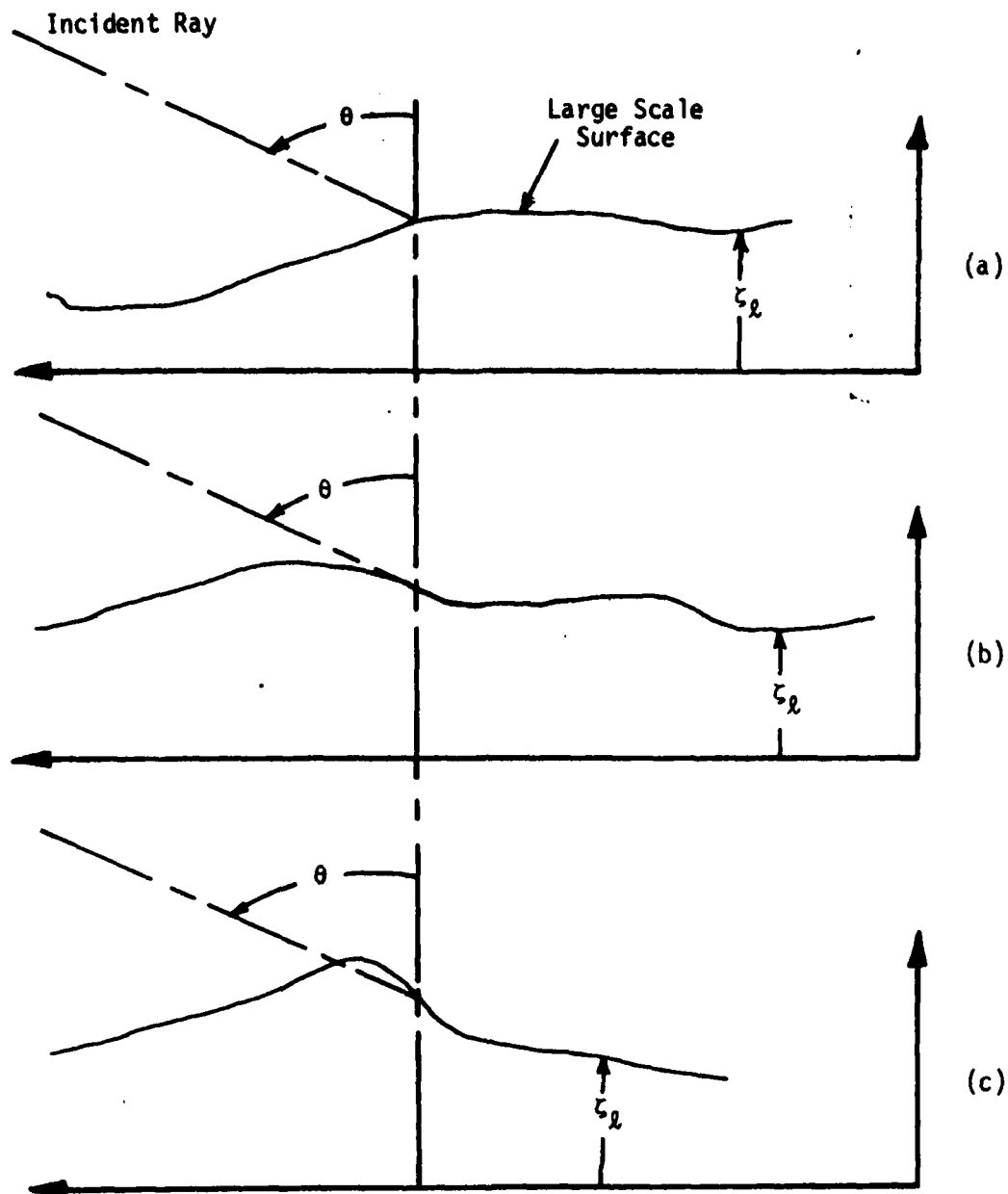


Figure 2-1. Diagrams explaining the reason for the unit step function in the shadowing function. Only portions of the large scale surface are shown since the small scale structure does not impact the shadowing.

at the point of intersection. In this case the point may or may not be shadowed in a small neighborhood of the point depending upon the surface curvature. In (c), the surface slope exceeds the slope of the incident ray and the ray is necessarily shadowed by some portion of the surface in a small neighborhood of the point. Thus all points on the surface for which the slope, in the direction of the incident ray projected onto mean plane, exceeds the slope of the incident ray will be shadowed. Stated another way, the probability of such an event is one. This is the physical reason for the unit step function in (2.4) and subsequent equations involving the shadowing function.

In order to retain the physical significance of the unit step function, it is desirable to deal with a particular form of the equation for  $[\sigma_{pp}^0, (\theta, \phi)]_1$ , i.e. equation (40) of [1],

$$\begin{aligned}
 [\sigma_{pp}^0, (\theta, \phi)]_1 = & \frac{4k_o^4 (1 + C_o)^{-1}}{\pi \sqrt{\zeta_{\ell x}^2 \zeta_{\ell y}^2}} \int_{-\infty}^{\infty} \int_{-\infty}^{\infty} S(2k_o \cos \theta \xi_x + k_{ox}, 2k_o \cos \theta \xi_y + k_{oy}) \\
 & \cdot U(\cot \theta + \xi_x \cos \phi + \xi_y \sin \phi) \Gamma_{pp}^2(-\xi_x, -\xi_y) \\
 & \cdot \exp \left[ -\frac{\xi_x^2}{2\zeta_{\ell x}^2} - \frac{\xi_y^2}{2\zeta_{\ell y}^2} \right] d\xi_x d\xi_y - I_{k_d}
 \end{aligned} \tag{2.7}$$

where  $I_{k_d}$  is defined in [1]. Equation (2.7) expresses the convolutional broadening of the spectrum about the Bragg wavenumbers  $k_{ox}$  and  $k_{oy}$  as a direct consequence of the distribution of large scale slopes; that is,  $\xi_x$  and  $\xi_y$  are equivalent to  $\zeta_{\ell x}$  and  $\zeta_{\ell y}$ . It should be pointed out that the correct expression for the shadowing function has been used in (2.7). The curve in the  $\xi_x \xi_y$ -plane separating the regions where the step function is

zero and one is a straight line, i.e.  $\xi_x \cos \phi + \xi_y \sin \phi = -\text{ctn} \theta$ . Except for special values of  $\phi$  given in Table I, the step function in (2.7) will consequently give rise to a coupling between the  $\xi_x$  and  $\xi_y$  integrals. More specifically, the lower (upper) limit on the  $\xi_x$  integral in (2.7) is given by

$$\xi_x = \frac{-(\text{ctn} \theta + \xi_y \sin \phi)}{\cos \phi} \quad (2.8)$$

for  $\cos \theta > 0$  ( $< 0$ ). From an analytical point of view (2.8) represents an irritating consequence of shadowing. From a practical standpoint, the restrictions imposed by (2.8) may not be numerically relevant for a large range of incidence angles as demonstrated by the following argument. The dominant factor in the integrand in (2.7) is the slope dependent Gaussian term which is equivalent to the probability density function for the large scale slopes. For most practical purposes, the effect of this term is to truncate the range of integration in (2.7) to about a  $\pm 3$ -sigma excursion from  $\xi_x = \xi_y = 0$ . The  $\pm 3$ -sigma excursions for  $\xi_x$  and  $\xi_y$  are  $\pm 3\sqrt{\zeta_{\ell x}^2}$  and  $\pm 3\sqrt{\zeta_{\ell y}^2}$ , respectively, and substituting these values in the unit step function argument yields the following requirement

$$\pm 3\sqrt{\zeta_{\ell x}^2} \cos \phi \pm 3\sqrt{\zeta_{\ell y}^2} \sin \phi > -\text{ctn} \theta \quad (2.9)$$

for the unit step function to be unity. If  $0 < \phi < \pi/2$ , the "worst case" situation occurs when  $\xi_x = -3\sqrt{\zeta_{\ell x}^2}$  and  $\xi_y = -3\sqrt{\zeta_{\ell y}^2}$  or

$$3\sqrt{\zeta_{\ell x}^2} \cos \theta + 3\sqrt{\zeta_{\ell y}^2} \sin \phi < \text{ctn} \theta \quad (2.10)$$

The worst case situation occurs when the left hand side of (2.9) is most negative. Thus for numerical purposes and all values of  $\theta$  satisfying (2.10), one can replace the infinite limits in (2.7) by  $\pm 3\sqrt{\zeta_{\ell x}^2}$  and  $\pm 3\sqrt{\zeta_{\ell y}^2}$ .

TABLE I

Integration Limits for Eqn. (2.7) and  
 $\phi$  a Multiple of  $\pi/2$

$\phi$	$\xi_x$ integration limits		$\xi_y$ integration limits	
	lower	upper	lower	upper
0	$-\text{ctn } \theta$	$\infty$	$-\infty$	$\infty$
$\pi/2$	$-\infty$	$\infty$	$-\text{ctn } \theta$	$\infty$
$\pi$	$-\infty$	$\text{ctn } \theta$	$-\infty$	$\infty$
$3\pi/2$	$-\infty$	$\infty$	$-\infty$	$\text{ctn } \theta$

Conditions similar to (2.10) can be obtained for other ranges of  $\phi$  in a straightforward manner.

It is implicitly assumed that the upper limit on  $\theta$  resulting from (2.10) also satisfies the optical criterion required of the large scale surface\*, namely that  $4k_0^2 \overline{\zeta_\ell^2} \cos^2 \theta \gg 1$ . For moderate slopes there will generally be a gap between the maximum value of  $\theta$  resulting from (2.10) and the upper bound on  $\theta$  resulting from the large scale surface optical criterion. In this case, one must necessarily revert to the more exact limits such as given by (2.8). What is happening in this situation is that the  $\pm 3$ -sigma support of the slope density function in (2.7) is overlapping the region of the  $\xi_x \xi_y$ -plane where the unit step function is zero. In fact, if one could go to the grazing incidence limit ( $\theta = \pi/2$ ), it is readily observed from Figure 2.2 that only half the  $\xi_x \xi_y$ -plane is encompassed by the integrals in (2.7). Thus, in addition to the attenuation of  $[\sigma_{pp}^0]_1$  near grazing incidence due to the  $(1+C_0)^1$  factor, there is another reduction factor resulting from the shadowing of points on the large scale surface having positive slopes (see Figure 2.1). It should be remembered that although the impact of the unit step function upon the limits of the integrals in (2.7) is somewhat involved, it is a direct consequence of the rather simple slope-shadowing limitations explained in Figure 2.1.

The analysis presented above does not alter the general composite surface scattering theory set forth in [1]. It does, however, correct and expand the theory in [1] as it relates to the effects of shadowing upon large angle of incidence backscattering from a randomly rough surface. This additional analysis was necessitated by the use of an incorrect functional form for the shadowing function in [1].

---

\*This criterion has also been called the stationary phase approximation [4] and the deep phase modulation condition [5].

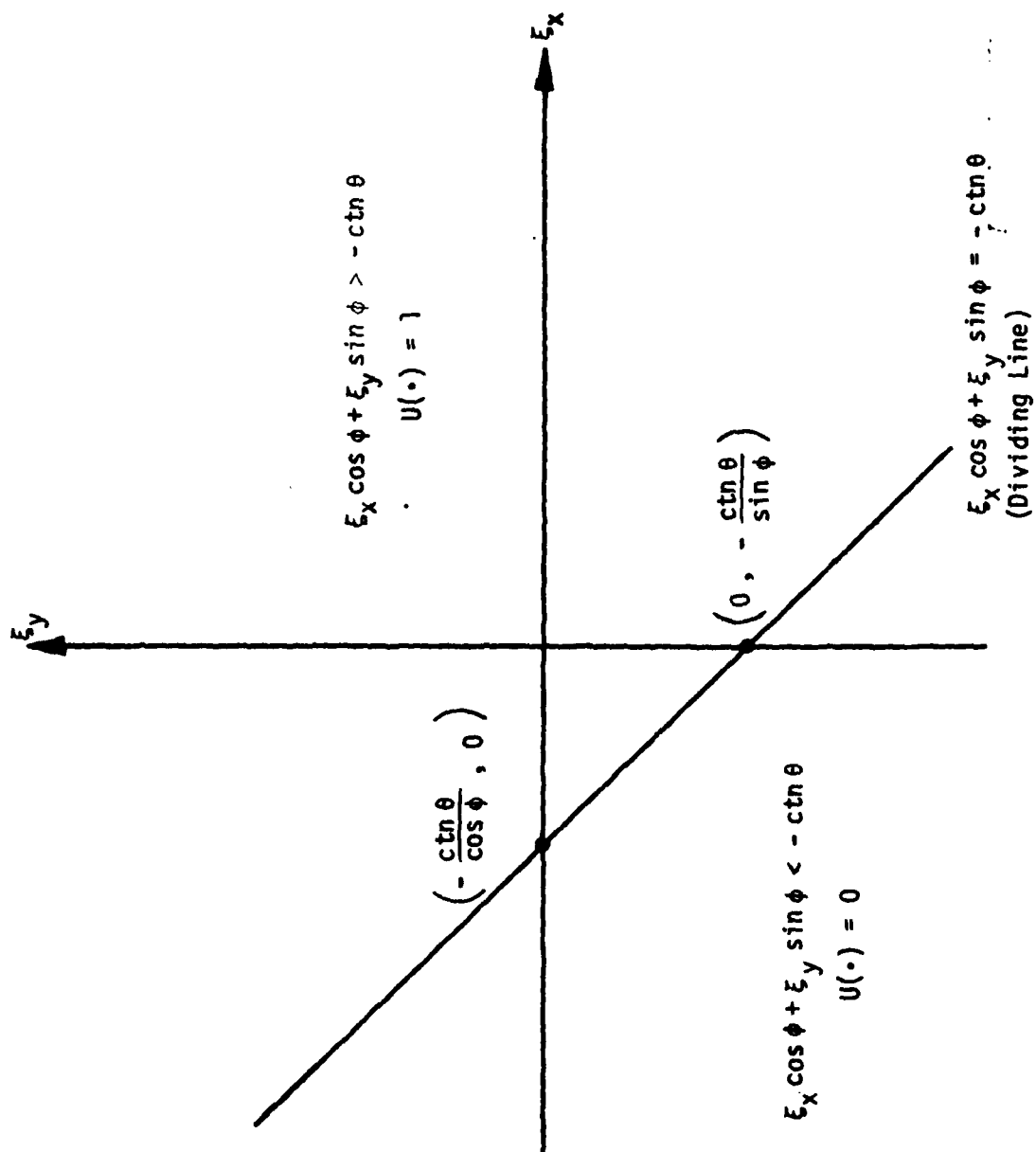


Figure 2-2. A plot of the regions in which the unit step function in the shadowing function is zero and unity.

## 2.4 Discussion of Numerical Example

The use of an incorrect shadowing function in Sections I through IV of [1] was primarily a sin of omission. That is, since nearly all the results in Section I through IV of [1] were formal in nature, it was not necessary to use the erroneous shadowing function given by (28) of [1]. However, the numerical example comprising Section V of [1] does require attention in order to properly account for the effects of large scale shadowing. In the example presented in [1],  $R$  was set equal to unity because the large scale slopes were relatively small. According to the analysis presented above, this step is not justified for all angles of incidence. The correct effect of shadowing is addressed below.

As in Section V of [1], it is assumed that  $\Gamma_{pp'}^2 \approx \Gamma_{pp'}^2(0,0)$  and the surface height spectrum is isotropic, i.e.  $\overline{\zeta_{lx}^2} = \overline{\zeta_{ly}^2} = \overline{\zeta_{lt}^2}/2$  and  $S(k_x, k_y) = S(\sqrt{k_x^2 + k_y^2})$ . Substituting  $k \cos \alpha = k_x$ ,  $k \sin \alpha = k_y$  and  $dk_x dk_y = k dk d\alpha$  in (32) of [1] and using (2.6) above for the shadowing function yields;

$$[\sigma_{pp'}^0]_1 = \frac{2k_o^2 \Gamma_{pp'}^2(0,0)}{\pi \overline{\zeta_{lt}^2} \cos^2 \theta (1 + C_o)} \int_0^{2\pi} \int_{k_d}^{\infty} S(k) U \left( \cot \theta + \tan \theta + \frac{k \cos(\alpha - \phi)}{2k_o \cos \theta} \right) \cdot \exp \left\{ - [4k_o^2 \sin^2 \theta + k^2 + 4kk_o \sin \theta \cos(\alpha - \phi)] / 4k_o^2 \overline{\zeta_{lt}^2} \cos^2 \theta \right\} k dk d\alpha \quad (2.11)$$

The unit step function is unity whenever  $k \cos(\alpha - \phi) > -2k_o / \sin \theta$ . Since the minimum value of  $\cos(\alpha - \phi)$  is -1, this inequality will be satisfied for all  $\alpha$  if  $k$  is restricted to less than  $2k_o / \sin \theta$ . Since the range of  $k$  from  $2k_o / \sin \theta$  to  $\infty$  for  $\cos(\alpha - \phi) > 0$  contributes little to the integral in (2.11) (because  $\overline{\zeta_{lt}^2}$  is small), the  $k$ -integral limits can be approximated by

$[k_d, 2k_o/\sin \theta]$ . In this range of  $k$ , the step function is unity and the  $\alpha$ -integration can be accomplished with the following result;

$$[\sigma_{pp'}^o]_1 \approx \frac{4k_o^2 \Gamma_{pp'}^2(0,0)}{\zeta_{lt}^2 \cos^2 \theta (1+C_o)} \int_{k_d}^{2k_o/\sin \theta} S(k) I_o \left( \frac{k \sin \theta}{k_o \zeta_{lt}^2 \cos^2 \theta} \right) \exp \left\{ - \frac{(k-2k_o \sin \theta)^2}{4k_o^2 \zeta_{lt}^2 \cos^2 \theta} - \frac{k \sin \theta}{k_o \zeta_{lt}^2 \cos^2 \theta} \right\} k dk \quad (2.12)$$

where  $I_o(\cdot)$  is a Bessel function of the second kind. The right hand side of (2.12) may now be compared with the  $[\sigma_{pp'}^o]_1$  part in (44) of [1], i.e.

$$\frac{4k_o^2 \Gamma_{pp'}^2(0,0)}{\zeta_{lt}^2 \cos^2 \theta} \int_{k_d}^{\infty} S(k) I_o \left( \frac{k \sin \theta}{k_o \zeta_{lt}^2 \cos^2 \theta} \right) \exp \left\{ - \frac{(k-2k_o \sin \theta)^2}{4k_o^2 \zeta_{lt}^2 \cos^2 \theta} - \frac{k \sin \theta}{k_o \zeta_{lt}^2 \cos^2 \theta} \right\} k dk \quad (2.13)$$

The obvious differences are the factor  $(1+C_o)^{-1}$  and the finite upper limit on the integral in (2.12). Figure 2.3 illustrates how  $(1+C_o)^{-1}$  varies with  $\theta$  for  $\zeta_{lt}^2 = 0.0224$  which was the value of mean square slope used to construct Figures 3 and 4 of [1]. Of particular note in the plot of  $(1+C_o)^{-1}$  is the fact it does not start to decrease until  $\theta$  exceeds  $85^\circ$ ; at  $87.5^\circ$   $(1+C_o)^{-1} = -2.5$  dB. The value of  $\theta = 87.5^\circ$  is the point at which  $4k_o^2 \zeta_{lt}^2 \cos^2 \theta \approx 10$  and, consequently, represents the approximate limit of the large scale theory. That is, for  $\theta > 87.5^\circ$  the analysis of the scattering from the large scale structure on the surface can no longer be accomplished using optical techniques. The effect of the finite upper limit on the integral in (2.12) is much less dramatic. In fact if the  $4k_o^2 \zeta_{lt}^2 \cos^2 \theta \gtrsim 10$  criterion is ignored and the limit

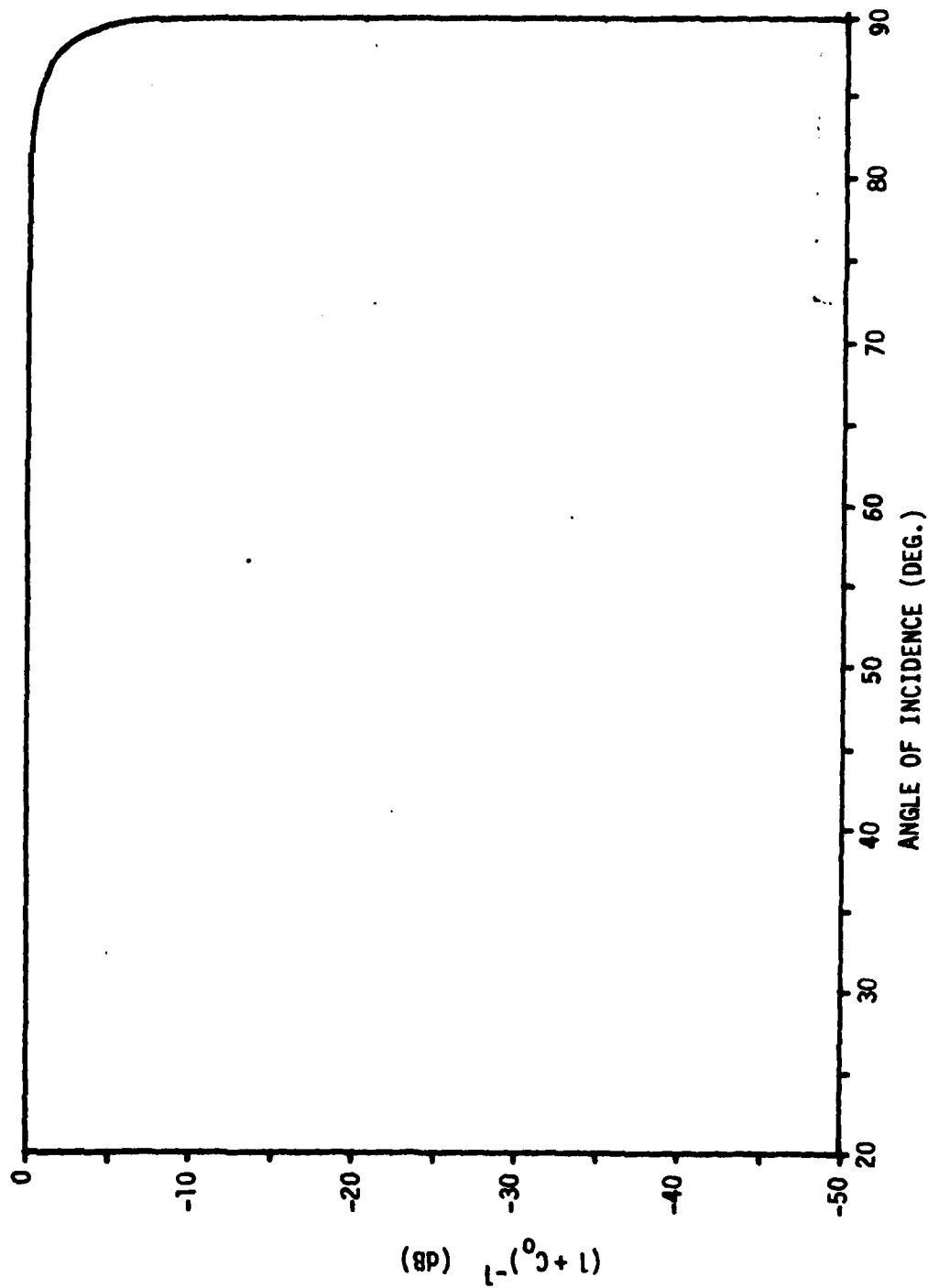


Figure 2-3. Behavior of the factor  $(1 + C_0)^{-1}$  resulting from the corrected shadowing function for  $\zeta_{0x}^2 = 0.0224$ .

of  $\theta = 90^\circ$  is taken in (2.12), it can be shown\* that the finite upper limit gives rise to a 3 dB reduction from the value of (2.13) at  $\theta = 90^\circ$ . This same conclusion can also be obtained from (2.7) and it is a direct consequence of the fact that all positive slopes are excluded from consideration at  $\theta = 90^\circ$  (see Figure 2.1). Within the range of validity of the optical criterion, the finite upper limit on the integral in (2.12) gives rise to much less attenuation than the  $(1+C_0)^{-1}$  factor.

In view of the above analysis, it is concluded that the numerical results presented in Section V of [1] are correct as they were presented. Determination of the spectral division wavenumber  $k_d$  is in no way altered by the inclusion of the correct shadowing function. The curves shown in Figures 3 through 6 of [1] are correct because they do not encompass the range of  $\theta$  where shadowing is important ( $\theta \gtrsim 85^\circ$ ). As noted above, the onset of shadowing effects occurs approximately where the optical criterion ( $4k_o^2 \zeta_\ell^2 \cos^2 \theta \gtrsim 10$ ) is violated, i.e.  $\theta \approx 87.5^\circ$ , for the numerical example presented in [1]. However, for larger slopes shadowing must be considered since it will cause a significant reduction in  $\sigma_{pp}^o$ , near grazing incidence.

## 2.5 Summary

In the analysis presented in [1], it was correctly demonstrated how one includes the effects of large scale surface feature shadowing on the backscattering cross section of a composite surface for large angles of incidence. Unfortunately, an incorrect form for the shadowing function was used in [1] which led to the erroneous evaluation of the impact of shadowing upon large angle of incidence scattering. In this section, the correct form of the shadowing

---

\*To show this one can apply Laplace's method to asymptotically evaluate (2.12) as  $\cos \theta \rightarrow 0$ . However, it must be remembered that the maximum of the integrand occurs at the upper limit of the integrand as  $\cos \theta \rightarrow 0$  and this impacts the evaluation of the integral [6].

function has been presented and included in the formulas obtained in [1]. Particular emphasis has been placed upon the physical significance of shadowing as it effects large angle of incidence scattering. It has been shown that shadowing leads to multiplication of both  $[\sigma_{pp}^0]_0$  and  $[\sigma_{pp}^0]_1$  by the factor  $(1+C_0)^{-1}$  which causes  $[\sigma_{pp}^0]_1$  and, thus,  $\sigma_{pp}^0$  to go to zero near grazing incidence for a perfectly conducting, randomly rough, composite surface. Furthermore, there is another effect which leads to an additional 3 dB attenuation at grazing incidence ( $\theta = 90^\circ$ )\*. This effect results from those slopes which, with probability one, will cause the point on the surface having these slopes to be shadowed. At grazing incidence, all positive slopes are in this class.

A reevaluation of the numerical results presented in [1] revealed that use of the correct shadowing function did not alter any of the results relative to the choice of the spectral dividing wavenumber  $k_d$ . Furthermore, none of the curves presented in [1] were effected because they only encompass the range of  $\theta$  from 0 to  $70^\circ$  and the effects of shadowing were present for  $\theta \geq 85^\circ$ . Also, techniques were presented relative to overcoming some of the analytical difficulties resulting from the use of the correct shadowing function.

---

\*It is reemphasized that exact grazing incidence cannot be addressed by this theory because the optical criterion assumed of the large scale surface features is violated. The -3 dB figure is significant only in its magnitude relative to the effect of the  $(1+C_0)^{-1}$  factor.

### References

1. Brown, G. S., "Backscattering from a Gaussian-distributed perfectly conducting rough surface," IEEE Trans. Antennas & Propg., AP-26, pp. 472-82 May, 1978.
2. Sancer, M. I., "Shadow-Corrected electromagnetic scattering from a randomly rough surface," IEEE Trans. Antennas & Propg., AP-17, pp. 577-585, September, 1969.
3. Smith, G. B., "Geometrical shadowing of a random rough surface," IEEE Trans. Antennas & Propg., AP-15, pp. 668-71, September, 1967.
4. Kodis, R. D., "A note on the theory of scattering from an irregular surface," IEEE Trans. Antennas & Propg., AP-14, pp. 77-82, January, 1966.
5. Hagfors, T., "Relationship of geometric optics and autocorrelation approach to the analysis of lunar and planetary radar," J. Geophys. Res., 71, No. 4, pp. 379-83, 1966.
6. Erdelyi, A., Asymptotic Expansions, Dover Publications, New York, Section 24, 1956.

### 3.0 SHADOWING BY NON-GAUSSIAN RANDOM SURFACES

#### 3.1 Background

Shadowing of random surfaces was originally introduced [1] as an ad hoc correction to the results provided by physical or geometrical optics approximate theories of rough surface scattering. Sancer [2] subsequently demonstrated how shadowing could be rigorously accounted for in the optical limit for random surfaces. Furthermore, he showed that previously derived expressions for the effects of shadowing based upon purely geometrical considerations [3, 4] were directly applicable. Using Sancer's results, Brown [5,6] showed how shadowing could be rigorously included in a formulation for scattering from random surfaces characterized by many scales of roughness, i.e. composite rough surfaces.

While shadowing theory is reasonably mature, it has only been applied to jointly Gaussian random surfaces. The Gaussian results are probably adequate for the ocean but they are questionable for terrain and completely inadequate for sea ice fields. For sea ice, water first fills all surface depressions below mean sea level and then freezes. This eliminates all surface height excursions below mean sea level and the probability density function of the surface roughness is clearly non-Gaussian. For these reasons, it is important to extend shadowing theory to the point where it can easily accommodate non-Gaussian surface statistics; such is the purpose of this section.

#### 3.2 Analysis

The special case of backscattering is chosen to illustrate the approach; this minimizes some of the conceptual details associated with the more general bistatic case. It turns out that the extension of the results to the bistatic geometry can be accomplished almost by inspection. The analysis presented by Smith [4] is general to a point in the development; however, there are a number

of integrations which must be accomplished in order to arrive at the final expression for the shadowing function. In the case of a jointly Gaussian surface these integrals can be performed and a closed-form result is obtained for the shadowing function. For non-Gaussian surfaces, the required integrations appear to be, at best, formidable. The purpose of this section is to show that if the height and slopes of the surface are independent random variables then the final expression for the shadowing function is drastically simplified.

For the reader's convenience Smith's notation will be employed in this section and his Figure 1 is essentially repeated here as our Figure 3.1. There are three critical relationships from Smith's paper [4] which are required. If  $S(F, \theta)$  is the probability that no part of the surface will intersect the incident ray (at an angle  $\theta$  with respect to the normal to the mean flat surface) on its way to point  $F$  on the surface then  $S(F, \theta)$  is given by

$$S(F, \theta) = h(\mu - q_0) \exp \left\{ - \int_0^{\infty} g(\tau) d\tau \right\} \quad (3.1)$$

where  $h(\cdot)$  is the unit step function,  $\mu = \cot \theta$ ,  $q_0$  is the slope of the surface in the  $y$ -direction at  $F$ , and  $g(\tau) d\tau$  is the conditional probability that the surface will intersect the incident ray in the interval  $(\tau, \tau + d\tau)$  given that it does not intersect the ray in  $(0, \tau)$ . The function  $g(\tau) d\tau$  is determined by the behavior of  $P_3(\xi, q | F, \tau)$  which is the joint probability of the height  $\xi$  and  $y$ -slope at the point  $(x=0, y=\tau)$  conditioned upon the height  $(\xi_0)$  and  $y$ -slope  $(q_0)$  at point  $F$ ; in particular,

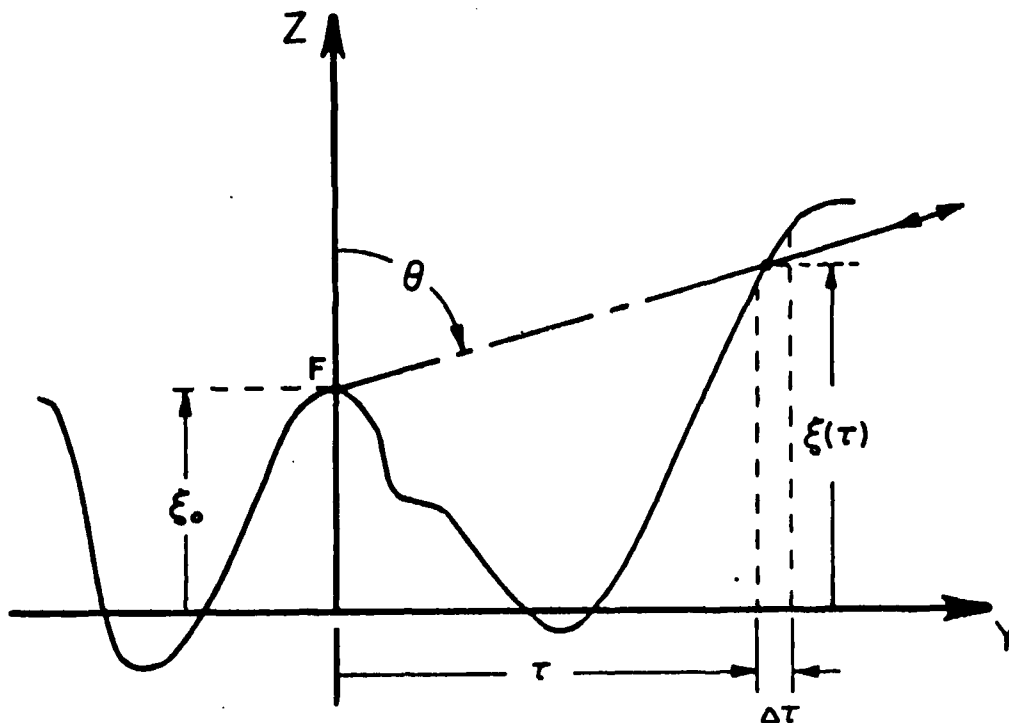


Figure 3-1. Shadowing geometry. The incident ray lies in the  $x = 0$  plane and the slopes of the surface at the point  $F$  are  $\partial \xi / \partial x = p_0$  and  $\partial \xi / \partial y = q_0$ .

$$g(\tau)\Delta\tau = \frac{\int_{-\infty}^{\infty} (q - \mu) P_3(\xi, q|F, \tau) \Big|_{\xi = \xi_0 + \mu\tau} dq}{\int_{-\infty}^{\infty} dq \int_{-\infty}^{\xi_0 + \mu\tau} P_3(\xi, q|F, \tau) d\xi} \Delta\tau \quad (3.2)$$

The average of  $S(F, \theta)$  over all surface heights with  $p_0 = 0$  and  $q_0 = -1/\mu$  is the desired shadowing function  $R(\theta)$ , i.e. the probability that a back-scattering specular point on the surface will not be shadowed.

Smith proceeded to evaluate (3.2) in the Gaussian case by assuming that the heights and slopes at  $F$  were uncorrelated with those at  $y = \tau$ . The same assumption will be made here. Furthermore, it will be assumed that the height and slopes are independent random variables; thus,

$$P_3(\xi, q|F, \tau) = P_1(\xi)P_2(q) \quad (3.3)$$

where  $P_1(\xi)$  is the height probability density function and

$$P_2(q) = \int_{-\infty}^{\infty} P_{22}(p, q) dp \quad (3.4)$$

where  $P_{22}(p, q)$  is the joint probability density function of the  $x$  and  $y$  slopes. Substituting (3.3) into (3.2) yields the following

$$g(\tau) = \frac{\Gamma P_1(\xi_0 + \mu\tau)}{\int_{-\infty}^{\xi_0 + \mu\tau} P_1(\xi) d\xi} \quad (3.5)$$

where

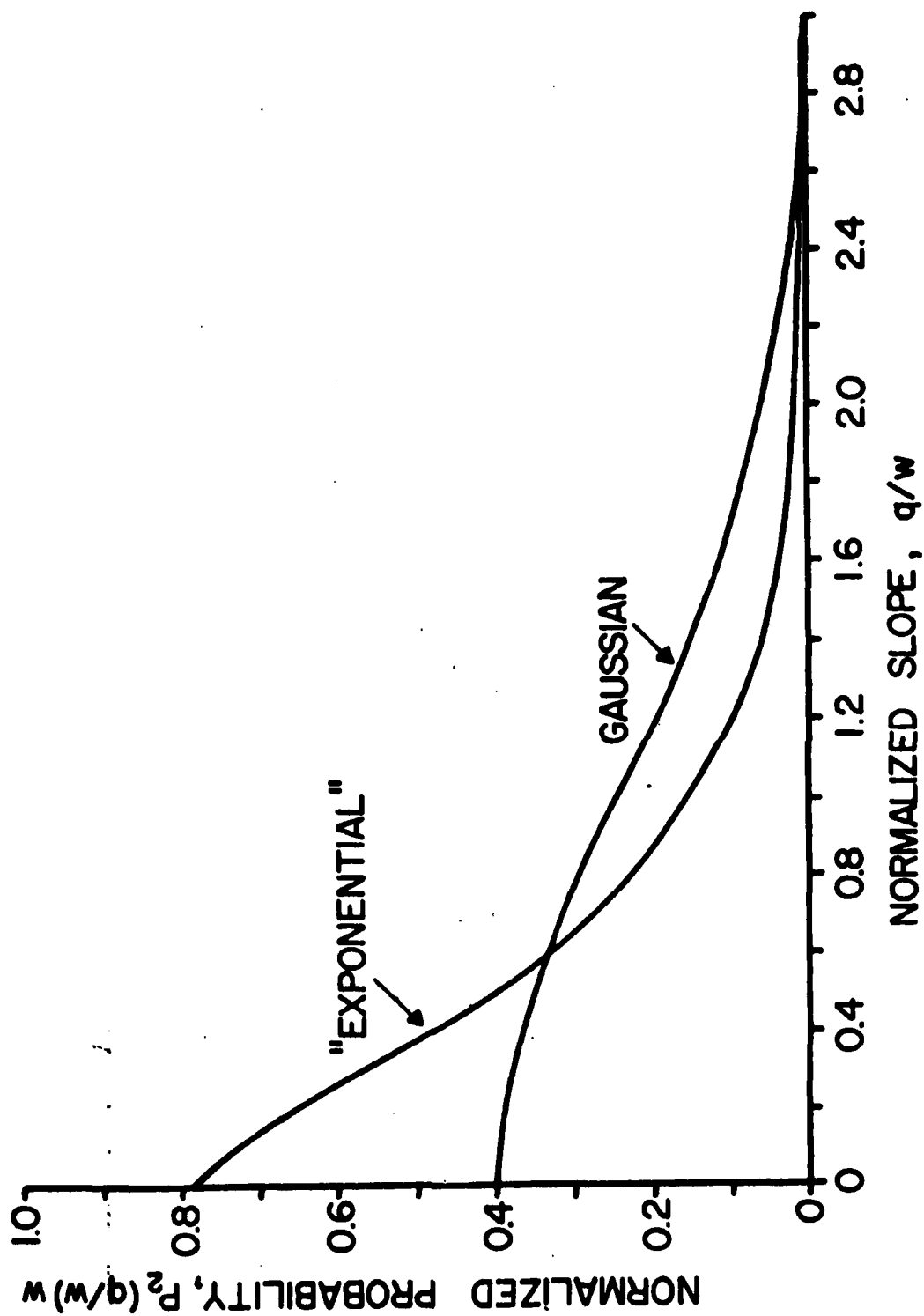


Figure 3-2. A comparison of the "exponential" marginal slope density given by (3.13) and the Gaussian.

$$\Gamma = \int_{\mu}^{\infty} (q - \mu) P_2(q) dq \quad (3.6)$$

The denominator of (3.5) is recognized as the distribution function for  $\xi$  evaluated at  $\xi_0 + \mu\tau$ , i.e.  $F_1(\xi_0 + \mu\tau)$ . Also,  $P_1(\xi_0 + \mu\tau)$  in (3.5) is equal to the derivative of the distribution function evaluated at  $\xi = \xi_0 + \mu\tau$ . Consequently, (3.5) becomes  $g(\tau) = [\Gamma/F_1(\xi_0 + \mu\tau)] dF_1(\xi_0 + \mu\tau)/d(\xi_0 + \mu\tau)$ . Substituting this result in (3.1), making the change of variable  $\eta = \xi_0 + \mu\tau$  and noting that  $dF_1/F_1 = d(\ln F_1)$  yields

$$S(\theta, F) = h(\mu - q_0) \exp \left\{ -\Gamma/\mu \int_{\eta = \xi_0}^{\infty} d[\ln F_1(\eta)] \right\} \quad (3.7)$$

where  $\ln$  denotes the natural logarithm. Since  $F_1(\infty) = 1$ , (3.7) reduces to the following;

$$S(\theta, F) = h(\mu - q_0) F_1(\xi_0)^{\Gamma/\mu}. \quad (3.8)$$

Remembering that  $P_1(\xi_0) = dF_1(\xi_0)/d\xi_0$ , the average of (3.8) over all values of  $\xi_0$  simplifies to

$$S(p_0, q_0, \theta) = h(\mu - q_0) \int_{\xi_0 = -\infty}^{\infty} \{F_1(\xi_0)\}^{\Gamma/\mu} dF_1(\xi_0) \quad (3.9)$$

or

$$S(p_0, q_0, \theta) = \frac{h(\mu - q_0)}{\Gamma/\mu + 1} \quad (3.10)$$

since  $F_1(-\infty) = 0$  and  $\Gamma/\mu + 1 \geq 0$ . With  $q_0 = -1/\mu$ , the shadowing function appropriate for backscatter reduces to the following simple expression;

$$R(\theta) = \left\{ 1 + \int_{\mu}^{\infty} (q/\mu - 1) P_2(q) dq \right\}^{-1} \quad (3.11)$$

where, in summary,  $\mu = \cot \theta$ ,  $\theta$  is the incidence angle, and  $P_2(q)$  is the probability density function of the slopes of the surface in the plane of incidence defined by the incident ray and the normal to the mean surface. It is interesting to note from (3.11) that for normal incidence ( $\theta = 0$ )  $R(0) = 1$  whereas at grazing incidence ( $\theta = \pi/2$ )  $R(\pi/2) = 0$  since  $\mu = 0$  and  $\int_0^{\infty} q P_2(q) dq > 0$ . Thus, these basic properties of the shadowing function are independent of the detailed properties of the slope density function. One can easily verify that (3.11) is identical to the results obtained by Smith for the special case of a jointly Gaussian surface.

The form of (3.10) compared to Smith's results, i.e. (23) of [4], suggests that the above result can be directly translated to the bistatic case and, indeed, this is the case. For the bistatic case, a generalization of Sancer's [2] results will be given. It should be noted that the inequalities involving the angles of incidence ( $\theta_0$ ) and scattering ( $\theta$ ), just prior to Sancer's equations (49), (50), (54) and (55) should be reversed. With  $\mu = \cot \theta$  and  $\mu_0 = \cot \theta_0$ , Sancer's results are easily generalized by replacing his  $C_0$  by  $\Gamma(\mu_0)/\mu_0$  and  $C_2$  by  $\Gamma(\mu)/\mu$ .

### 3.3 Example

To illustrate the above results, the backscattering shadowing function  $R(\theta)$  will be determined for the exponential joint slope density function introduced by Barrick [7], i.e.

$$P_{22}(p, q) = \frac{3}{\pi w^2} \exp \left[ - \sqrt{6(p^2 + q^2)/w^2} \right] \quad (3.12)$$

where  $w^2$  is the mean square slope of the surface roughness.  $P_{22}(p,q)$  in (3.12) represents a surface whose roughness is isotropic,  $w^2/2 = \langle p^2 \rangle = \langle q^2 \rangle$ , with statistically dependent slopes. That is, the joint density function cannot be expressed as a product of the marginal or individual densities. The calculation of the marginal density  $P_2(q)$ , using (3.4), is reasonably straightforward and the result is as follows;

$$P_2(q) = \frac{6}{\pi w^2} |q| K_1(\sqrt{6} |q|/w) \quad (3.13)$$

where  $K_1(\cdot)$  is one of the modified Bessel functions of order one [8]. It is interesting to compare this density with a Gaussian, i.e.

$$P_2(q) = \frac{1}{w\sqrt{2\pi}} \exp(-q^2/2w^2)$$

and this is done in Figure 3.2 where the normalized densities  $P_2(q)w$  are plotted as a function of the normalized slope  $q/w$ . It should be noted from the plots in Figure 3.2 that the "exponential" density shows a much greater probability of occurrence of small slopes than the Gaussian. This result is in agreement with one intuitive approach for generating a surface characterized by (3.12), e.g. one strongly filters all surface height excursions below a certain level to eliminate the possibility of large negative height excursions. This process increases the probability of small slopes at the expense of the large slopes.

Substituting (3.13) in (3.11) and using tabulated integrals of Bessel functions given in [9], the following closed-form result is obtained for the backscattering shadow function  $R(\theta)$  ;

$$R(\theta) = \left\{ \frac{\pi}{\pi} K_2(x) + \frac{1}{2} + \frac{x}{2} \left[ K_1(x)L_0(x) + L_1(x)K_0(x) \right] \right\}^{-1} \quad (3.14)$$

where  $x = (\sqrt{6}/w) \cot \theta$  and the  $L_n(\cdot)$ ,  $n=0$  or  $1$ , symbol denotes the modified Struve functions [8]. Using asymptotic forms for the special functions in (3.14), it may be readily verified that  $R(0) = 1(x \rightarrow \infty)$  and  $R(\pi/2) = 0(x=0)$ . The modified Struve functions may be computed from tables given in [8] for  $x \gtrsim 5$  and by a power series for smaller arguments.

Figure 3.3 compares (3.14) and the shadowing function for a Gaussian function obtained by Smith [4] for a range of rms slopes. The shadowing function for the exponential joint slope density is larger because the marginal slope density given by (3.13) exhibits less likelihood for large slopes than the corresponding Gaussian density. That is, the larger slopes are the source of more significant shadowing.

### 3.4 Summary

The shadowing theory developed by Smith [4], while sufficiently general to deal with any joint slope density function, involves what appears to be a number of rather complicated integrals. Under the assumption that the surface height is statistically independent of the surface slopes, it is shown that Smith's theory can be reduced to a single integration involving the marginal density function for the slopes in the plane of incidence. Using this result but without regard to the specific form of the marginal density function, it can be shown that the backscattering shadowing function is unity at normal incidence and zero at grazing incidence. Because the final result involves an integration or smoothing process, it is amenable to the use of histogram data for the marginal slope density.

This theory is applied to an exponential joint slope density representing an isotropic surface for which the slopes are not statistically independent. The backscattering shadowing function for the exponential and Gaussian joint slope densities are compared and it is found that the Gaussian surface

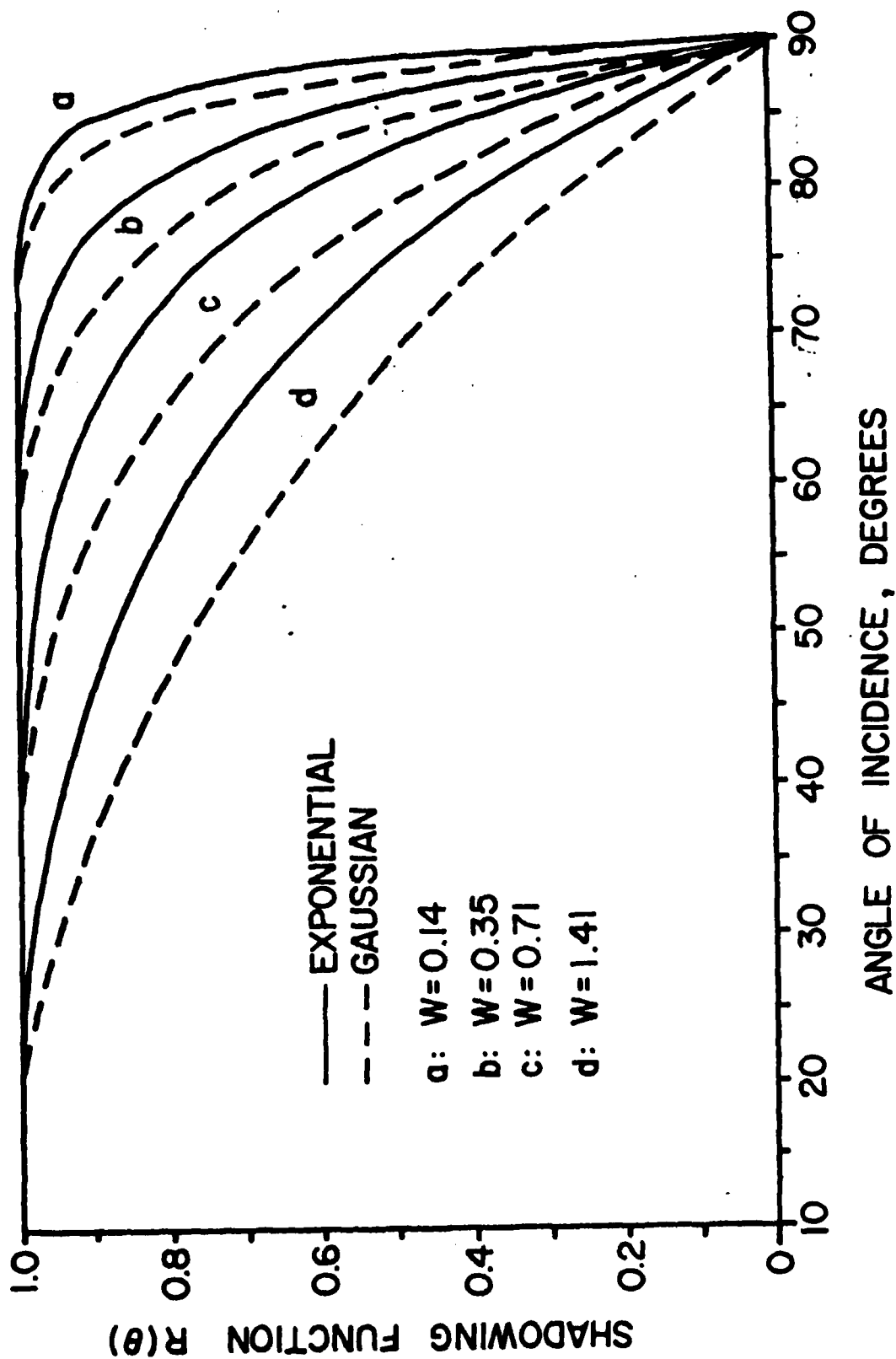


Figure 3-3. A comparison of the backscattering shadowing function for the exponential and Gaussian joint slope densities for a range of rms slopes ( $w$ ).

produces stronger shadowing. This result is found to be a consequence of the greater likelihood of large slopes with the Gaussian density.

#### References

1. Beckmann, P., "Shadowing of random rough surfaces, IEEE Trans. Antennas & Propag., Vol. AP-13, pp. 384-388, May 1965.
2. Sancer, M. I., "Shadow-corrected electromagnetic scattering from a randomly rough surface," IEEE Trans. Antennas & Propg., Vol. AP-17, pp. 577-585, September, 1969.
3. Wagner, R. J., "Shadowing of randomly rough surfaces," Report No. 7401-6012-R0000, TRW Systems Gp., Redondo Beach, CA., 1966.
4. Smith, B. G., "Geometrical shadowing of a random rough surface," IEEE Trans. Antennas & Propg., Vol. AP-15, pp. 668-671, Sept. 1967.
5. Brown, G. S., "Backscattering from a Gaussian-distributed perfectly conducting rough surface," IEEE Trans. Antennas & Propg., Vol. AP-26, pp. 472-482, May 1978.
6. Brown, G. S., "Corrections to 'Backscattering from a Gaussian-distributed perfectly conducting rough surface,' " IEEE Trans. Antennas & Propg., to be published.
7. Barrick, D. E., "Rough Surface Scattering Base On The Specular Point Theory," IEEE Trans. Antennas & Propg., Vol. AP-16, pp. 449-454, July 1968.
8. Abramowitz, M. and I. A. Stegun, Handbook of Mathematical Functions, Chs. 9 and 12, U. S. Govt. Printing Office, May 1968.
9. Gradshteyn, I. S. and I. M. Ryzhik, Tables of Integrals, Series, and Products, Academic Press, New York, 1965.

## 4.0 BISTATIC SCATTERING FROM LOSSY RANDOM SURFACES

### 4.1 Background

Prior to the mid-1960's, electromagnetic scattering from randomly rough surfaces was modeled using either perturbation theory or physical optics [1]. First order perturbation theory appeared to do a reasonable job of analytically describing the scattering process when the surface roughness was small in terms of the electromagnetic wavelength and multiple scattering was negligible. Physical optics produced meaningful results in and about the specular scattering direction when the surface exhibited very large but smoothly undulating height variations. Unfortunately, there were numerous attempts to apply these theories to situations where the implicit assumptions in the models were violated. These attempts usually assumed some surface parameter such that the scattering measurements and the "model" were brought into agreement. However, it was very quickly recognized that these attempts were highly suspect because of their failure to meet certain fundamental principles.

As more and more rough surface microwave scattering measurements were acquired, it became obvious that neither first order perturbation theory nor physical optics were individually adequate for all angles of incidence and scattering. Conversely, it appeared that physical optics seemed to do a good modeling job near the specular scattering direction while first order perturbation theory was reasonably accurate for all other scattering angles. Almost simultaneously, researchers in the U.S. [2] and the U.S.S.R. [3,4] began to advocate the combining of these two diverse theories in what was later to be called the composite surface scattering model. In this model, the surface was considered to be made up of both large and small scale surface features (height and spatial wavelength) relative to the electromagnetic wavelength,  $\lambda_0$ . The large scale surface features were considered to be responsible for

the physical optics-like scattering near the specular direction. The small scale surface structure gave rise to a perturbation field (to the optical field) which was the dominant scattering mechanism away from the specular scattering direction. The interaction between the optical and first order perturbation fields was assumed to be totally dependent upon the tilting of the small surface structure by the larger gently undulating features [5].

More recently, rigorous first order boundary perturbation theory has been applied to the problem of backscattering from a perfectly conducting, Gaussian distributed rough surface [6]. The results of this analysis indicated that much of the original work on this problem could be rigorously justified. Furthermore, additional insight was gained in regard to such aspects of the problem as shadowing (see Section 3 of this report), spectral dichotomy, and the tilting interpretation. A logical extension of this latter theory encompasses bistatic scattering from a lossy dielectric surface. The purpose of this section is to present the details associated with such an extension.

Before the details of scattering from a composite dielectric surface are presented, it is illuminating to consider two much simpler cases. The first is backscattering from a dielectric surface having only a small scale roughness while the second case addresses bistatic scattering. The advantages of this approach are that it leads to familiarity with the perturbation technique and it sets forth the principles that will be used for the composite surface.

#### 4.2 Backscattering From A Dielectric Surface With Small Scale Roughness

The geometry for this problem is shown in Figure 4-1. The mean or average surface is the  $z=0$  plane; the random roughness  $\zeta_s$  superposed upon this plane is positive for  $\zeta_s > 0$  and negative for  $\zeta_s < 0$ . Below the rough surface ( $z < \zeta_s$ ), the relative dielectric constant of the medium is  $\epsilon_r$  and the relative magnetic permeability is taken to be the same as for free-space,

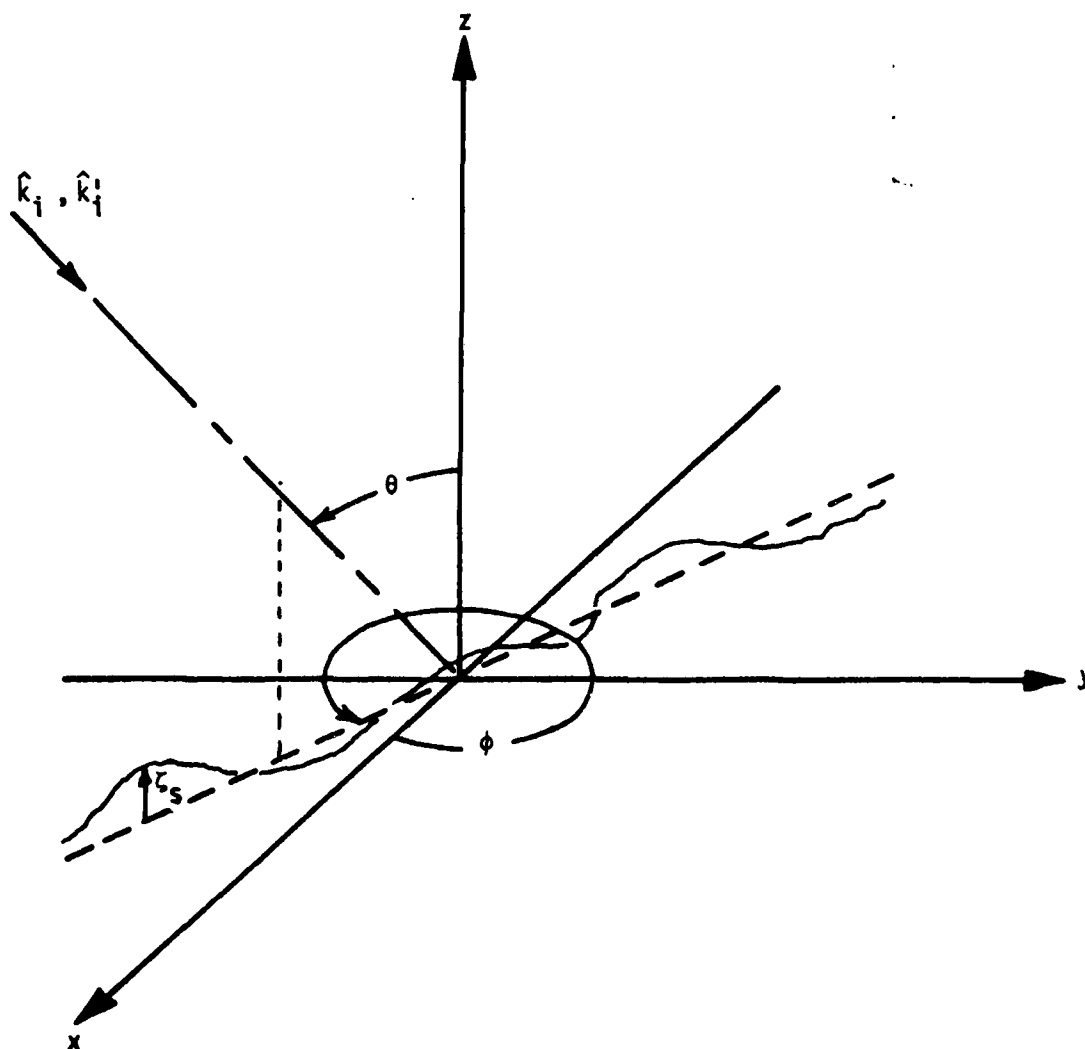


Figure 4-1. Geometry for backscattering from a randomly rough surface having only small scale roughness  $z_s$ .

i.e.  $\mu_r = 1$ . Above the rough surface ( $z > \zeta_s$ ), the medium is free-space,  
i.e.  $\epsilon_r = 1$  and  $\mu_r = 1$ .

Provided that the roughness is small with respect to the electromagnetic wavelength  $\lambda_0$ , e.g.  $4k_0^2 \overline{\zeta_s^2} \ll 1$  where  $k_0 = 2\pi/\lambda_0$  and  $\overline{\zeta_s^2}$  is the mean square height of the roughness, the scattered field  $\vec{E}^s$  can be expressed as follows;

$$\vec{E}^s \approx \delta^0 \vec{E} + \delta^1 \vec{E} \quad (4.1)$$

where  $\delta^0 \vec{E}$  is the field scattered by a surface having no roughness (the zeroth order perturbation) and  $\delta^1 \vec{E}$  is the scattered field which depends on the roughness to first order only (the first order perturbation). The primary assumption in (4.1) is that higher order terms such as  $O(\zeta_s^2)$ ,  $O(\zeta_s^3)$ , etc., are negligible. The zeroth order perturbation field  $\delta^0 \vec{E}$  is trivially determined since it is just the field reflected by an infinite, flat dielectric interface. Both Mitzner [7] and Burrows [8] have obtained particularly useful expressions for  $\delta^1 \vec{E}$ . The Mitzner result is more straightforward but it is restricted to small roughness perturbations superposed on a flat plane.<sup>①</sup> Burrows' solution for  $\delta^1 \vec{E}$  is somewhat more complicated but it is more general in that the unperturbed surface need not be planar or even deterministic. For small scale roughness on a plane, the Burrows formulation requires a bit more effort in computing  $\delta^1 \vec{E}$  than Mitzner's result. For a composite surface, only the Burrows result is sufficiently general to address this problem.

At first glance, the Burrows expression for  $\delta^1 \vec{E}$  appears to be somewhat cumbersome and confusing. However, if it is realized that the result is obtained

---

<sup>①</sup>Mitzner's result can actually be applied to any unperturbed surface for which the wave equation is separable. For the problem considered here, the surface is restricted to a plane.

from an application of reciprocity then the notation becomes more meaningful. Basically, one deals with two incident electric fields of the form

$$\vec{E}_i = E_i \hat{e} \quad E_i = E_o \exp(-j \vec{k}_i \cdot \vec{r}) \quad (4.2a)$$

and

$$\vec{E}_i' = E_i' \hat{e}' \quad E_i' = E_o \exp(-j \vec{k}_i' \cdot \vec{r}) \quad (4.2b)$$

where the primed field may have a different polarization and direction of incidence than the unprimed field. Burrows' expression for the first order perturbation (electric) field scattered in the direction  $-\hat{k}_i'$  and polarized in the  $\hat{e}'$  direction is as follows [8];

$$\delta^1 \vec{E} \cdot \hat{e}' = \frac{k_o^2 \exp(-jk_o R)}{4\pi R E_o \epsilon_o} \int_{S_o} [\Delta \vec{E} \cdot \vec{D}' + \Delta \vec{B} \cdot \vec{H}' - \Delta \vec{H} \cdot \vec{B}' - \Delta \vec{D} \cdot \vec{E}'] \zeta_s dS_o \quad (4.3)$$

where it is assumed that  $\delta^1 \vec{E} \cdot \hat{e}'$  is measured in the far-field of the rough surface. The distance  $R$  is measured from the origin of the reference coordinate system on the mean surface to the point of observation or measurement of  $\delta^1 \vec{E} \cdot \hat{e}'$  and  $\epsilon_o$  is the permittivity of free-space. The fields  $\vec{E}'$ ,  $\vec{H}'$ ,  $\vec{D}'$  and  $\vec{B}'$  are the fields on the unperturbed surface ( $S_o$ ) due to the primed incident field while  $\Delta \vec{E}$ ,  $\Delta \vec{H}$ ,  $\Delta \vec{D}$  and  $\Delta \vec{B}$  are the discontinuities in the fields on the unperturbed surface ( $S_o$ ) due to the unprimed incident field. Thus, to determine the  $\hat{e}_p$ -polarized component of the scattered first order perturbation field in the general direction  $\hat{k}_s$  one merely sets  $\hat{e}' = \hat{e}_p$  and  $\hat{k}_i' = -\hat{k}_s$  in the expression for the primed incident field  $\vec{E}_i'$ , computes the resulting fields  $\vec{E}'$ ,  $\vec{H}'$ ,  $\vec{D}'$ ,  $\vec{B}'$  on the unperturbed surface  $S_o$ , and substitutes these results in (4.3).

For backscattering  $\hat{k}_s = -\hat{k}_i$  so according to the above recipe,  $\hat{k}_i' = \hat{k}_i$

which in the coordinates of the geometry shown in Figure 4-1 is as follows;

$$\hat{k}_1' = \hat{k}_1 = k_0 (-\sin \theta \cos \phi \hat{x} - \sin \theta \sin \phi \hat{y} - \cos \theta \hat{z}) \quad (4.4)$$

Contrary to previous analyses [1], the direction of incidence specified by the angle  $\phi$  should not, at this point in the development, be arbitrarily set to some convenient value such as 0 or  $\pi/2$ . The reason for this is that the surface may have anisotropic roughness and the orientation of the  $x$  and  $y$  axes of the reference coordinate system should be fixed relative to this surface characteristic and not the direction of incidence.

Since the fields inside the surface integral in (4.3) are the fields induced on the infinite planar dielectric surface  $S_0$ , it is convenient to further categorize the problem according to the polarization of the incident fields. For both  $\vec{E}_1$  and  $\vec{E}_1'$  horizontally polarized,  $\hat{e}$  and  $\hat{e}'$  are orthogonal to the plane formed by the unit vectors  $\hat{k}_1$  and  $\hat{n} = \hat{z}$  where  $\hat{n}$  is the normal to the mean or unperturbed surface. In this case both  $\hat{e}$  and  $\hat{e}'$  are totally tangential to the mean plane. For both  $\vec{E}_1$  and  $\vec{E}_1'$  vertically polarized,  $\hat{e}$  and  $\hat{e}'$  are parallel to the plane formed by  $\hat{k}_1$  and  $\hat{n} = \hat{z}$ .

#### 4.2.1 Horizontal Polarization

When  $\hat{e}$  and  $\hat{e}'$  are tangential to the mean or unperturbed surface, the fields  $\vec{E}$ ,  $\vec{E}'$ ,  $\vec{D}$  and  $\vec{D}'$  (when evaluated on  $S_0$ ) are entirely tangential to  $S_0$ . Since the tangential component of the electric field is continuous across an interface,  $\Delta \vec{E} = 0$ . Furthermore, since there is no change in  $\mu_r$  across the boundary and the lower medium is assumed not to be perfectly conducting,  $\Delta \vec{B}$  and  $\Delta \vec{H}$  are both zero on the interface. Consequently, (4.3) reduces to the following;

$$\delta \vec{E} \cdot \hat{e}' = - \frac{k_o^2 \exp(-jk_o R)}{4\pi R E_o \epsilon_o} \int_{S_o} (\Delta \vec{D} \cdot \vec{E}') \zeta_s dS_o \quad (4.5)$$

The total  $\vec{E}'$ -field on the surface  $S_o$  due to  $\vec{E}_1'$  is given by

$$(1 + R_h) \vec{E}_1'(S_o) = E_o (1 + R_h) \exp(-j \vec{k}_1 \cdot \vec{r}_\perp) \hat{e}' \quad (4.6)$$

where  $R_h$  is the Fresnel (field) reflection coefficient for horizontal polarization and  $\vec{r}_\perp = x\hat{x} + y\hat{y}$  or just  $\vec{r}$  evaluated on  $S_o$ . The discontinuity in  $\vec{D}$  is given by

$$\Delta \vec{D} = \epsilon_o \left\{ \vec{E}_1(z=0^+) - \epsilon_r \vec{E}_1(z=0^-) \right\} \quad (4.7)$$

and

$$\vec{E}(z=0^+) = (1 + R_h) \vec{E}_1(S_o) \quad (4.8a)$$

$$\vec{E}(z=0^-) = T_h \vec{E}_1(S_o) \quad (4.8b)$$

where  $T_h$  is the Fresnel (field) transmission coefficient for horizontal polarization. Combining (4.8a) and (4.8b) in (4.7) yields

$$\Delta \vec{D} = \epsilon_o [1 + R_h - \epsilon_r T_h] \vec{E}_1(S_o)$$

or

$$\Delta \vec{D} = \epsilon_o [1 + R_h - \epsilon_r T_h] E_o \exp(-j \vec{k}_1 \cdot \vec{r}_\perp) \hat{e}' \quad (4.9)$$

Multiplying (4.7) by (4.9) and realizing that  $T_h = 1 + R_h$  yields

$$\Delta \vec{D} \cdot \vec{E}' = -\epsilon_o E_o^2 (1 + R_h)^2 (\epsilon_r - 1) \exp(-j 2 \vec{k}_1 \cdot \vec{r}_\perp) (\hat{e} \cdot \hat{e}') \quad (4.10)$$

Substituting this result in (4.5) produces the desired result for the first order perturbation field polarized in the  $\hat{e}'$  direction

$$\delta^1 \vec{E} \cdot \hat{e}' = \frac{k_o^2 E_o}{4\pi R} \exp(-j k_o R) (1 + R_h)^2 (\epsilon_r - 1) \iint \exp(-j 2 \vec{k}_1 \cdot \vec{r}_1) \zeta_s dx dy \quad (4.11)$$

where  $\hat{e} \cdot \hat{e}' = 1$ ,

$$R_h = \frac{\cos \theta - \sqrt{\epsilon_r - \sin^2 \theta}}{\cos \theta + \sqrt{\epsilon_r - \sin^2 \theta}}$$

and so

$$(1 + R_h)^2 (\epsilon_r - 1) = \frac{4(\epsilon_r - 1) \cos^2 \theta}{\left[ \cos \theta + \sqrt{\epsilon_r - \sin^2 \theta} \right]^2} \quad (4.12)$$

There are several points to note about (4.11). The derivation of (4.11) was considerably simpler than the Rayleigh-Rice approach [1]; this is because all of the difficult work was done in obtaining (4.3). Equation (4.7) is an expression for the scattered first order perturbation field, a more meaningful quantity than the average scattered power when dealing with phase sensitive systems. The average of (4.11) is zero because  $\langle \zeta_s \rangle = 0$ ; however, the average of  $\langle |\delta^1 \vec{E} \cdot \hat{e}'|^2 \rangle$  or the incoherent power is not zero. At the beginning of this section  $\hat{e}'$  was specified to be in the same direction as  $\hat{e}$ , thus  $\delta^1 \vec{E} \cdot \hat{e}'$  represents  $\delta^1 E_{hh}$  where the double-h subscript denotes horizontal polarization on transmission and reception. It is now possible to examine the consequences of cross-polarized sampling of the scattered field. In this case  $\hat{e}'$  is orthogonal to  $\hat{e}$ ; thus,  $\hat{e}$  is horizontally polarized and  $\hat{e}'$  is vertically polarized, i.e.

$$\hat{e} = \hat{e}_h = \sin \phi \hat{x} + \cos \phi \hat{y}$$

$$\hat{e}' = \hat{e}_v = -\cos \theta \cos \phi \hat{x} - \cos \theta \sin \phi \hat{y} + \sin \theta \hat{z}$$

Returning to (4.3) for this case, it is noted that  $\vec{\Delta E}$  is still zero because  $\vec{E}_1$  is tangential to  $S_0$ ,  $\vec{\Delta B}$  and  $\vec{\Delta H}$  are still zero because there is no change in  $\mu_r$  across  $S_0$  and the conductivity is assumed finite, and the problem reduces to evaluating  $\vec{\Delta D} \cdot \vec{E}'$  on  $S_0$ . However,  $\vec{\Delta D}$  has the direction  $\hat{e}_h$  while  $\vec{E}'$  is polarized in the  $\hat{e}_v$  direction, consequently,  $\hat{e} \cdot \hat{e}' = \hat{e}_h \cdot \hat{e}_v = 0$  and there is no depolarization by the surface. This is just a confirmation of the fact that first order perturbation theory does not lead to a depolarized scattered field when the roughness is small scale.

#### 4.2.2 Vertical Polarization

The case of vertical polarization is a bit more algebraically involved because  $\vec{\Delta E}$  is no longer zero across  $S_0$ . Both magnetic field discontinuities,  $\vec{\Delta B}$  and  $\vec{\Delta H}$ , are still zero for the same reason as given above.

Thus, (4.3) reduces to

$$\delta^1 \vec{E} \cdot \hat{e}' = \frac{k_o^2 \exp(-j k_o R)}{4\pi R E_o \epsilon_o} \int_{S_0} [\vec{\Delta E} \cdot \vec{D}' - \vec{\Delta D} \cdot \vec{E}'] \zeta_s dS_0 \quad (4.13)$$

For vertical polarization, it is customary to use the incident magnetic field  $\vec{H}_1$  as the source. Thus, the incident, reflected and transmitted magnetic fields on  $S_0$  are given by

$$\begin{aligned} \vec{H}_1 &= H_o \hat{e}_h \exp(-j \vec{k}_1 \cdot \vec{r}_1) \\ \vec{H}_r &= H_o R_v \hat{e}_h \exp(-j \vec{k}_r \cdot \vec{r}_1) \\ \vec{H}_t &= H_o T_v \hat{e}_h \exp(-j \vec{k}_t \cdot \vec{r}_1) \end{aligned}$$

where  $R_v$  and  $T_v$  are the Fresnel (field) reflection and transmission coefficients for vertical polarization. On  $S_0$  the corresponding electric fields are as follows;

$$\vec{E}_q = -\sqrt{\frac{\mu_0}{\epsilon_0}} \hat{k}_q \times \vec{H}_q \quad ; \quad E_t = -\sqrt{\frac{\mu_0}{\epsilon_0 \epsilon_r}} \hat{k}_t \times \vec{H}_t$$

where  $q = i, r$  and  $\hat{k}_i, \hat{k}_r$  and  $\hat{k}_t$  specify the direction of propagation of the incident, reflected, and transmitted fields. Note that since  $\vec{r}_\perp$  is on  $S_0$ ,

$$\vec{k}_i \cdot \vec{r}_\perp = \vec{k}_r \cdot \vec{r}_\perp = \vec{k}_t \cdot \vec{r}_\perp$$

which is merely a restatement of the fact that the angle of incidence equals the angle of reflection and Snell's law [9]. For backscattering and like polarization sampling of the scattered field, the primed fields are the same as those above.

Although somewhat cumbersome at this stage of the development, it is desirable to split the fields into components which are tangential to and normal to  $S_0$ . The reason for introducing this transformation is that it will be very useful in the composite surface development and it is therefore beneficial to obtain some facility with the technique on this easier problem. The normal to  $S_0$  is  $\hat{n} = \hat{z}$  while the tangent will be taken as  $\hat{\tau} = \hat{n} \times \hat{e}_h$ . This particular choice of  $\hat{\tau}$  is convenient because  $\hat{\tau} \cdot \hat{e}_v$  selects the component of  $\hat{e}_v$  that is tangent to the surface. Since  $\Delta \vec{E} \cdot \hat{\tau} = 0$  and  $\Delta \vec{D} \cdot \hat{n} = 0$  on  $S_0$ , (4.13) simplifies to

$$\delta^1 \vec{E} \cdot \hat{e}_v = \frac{k_0^2 \exp(-j k_0 R)}{4\pi R \epsilon_0 \epsilon_r} \int_{S_0} [(\Delta \vec{E} \cdot \hat{n})(\vec{D}' \cdot \hat{n}) - (\Delta \vec{D} \cdot \hat{\tau})(\vec{E}' \cdot \hat{\tau})] \zeta_s dS_0 \quad (4.14)$$

where  $\hat{e}'$  has been replaced by its equivalent  $\hat{e}_v$  since like polarization sampling of the scattered field has been specified. The boundary conditions  $\Delta \vec{E} \cdot \hat{\tau} = 0$  and  $\Delta \vec{D} \cdot \hat{n} = 0$  should not be discarded because they will provide some useful relationships. From  $\Delta \vec{E} \cdot \hat{\tau} = 0$  there results

$$[(\hat{k}_i \times \hat{e}_h) + R_v (\hat{k}_r \times \hat{e}_h)] \cdot \hat{\tau} = \frac{T_v}{\sqrt{\epsilon_r}} (\hat{k}_t \times \hat{e}_h) \cdot \hat{\tau} \quad (4.15)$$

while  $\Delta \vec{D} \cdot \hat{n} = 0$  yields

$$[(\hat{k}_i \times \hat{e}_h) + R_v (\hat{k}_r \times \hat{e}_h)] \cdot \hat{n} = \sqrt{\epsilon_r} T_v (\hat{k}_t \times \hat{e}_h) \cdot \hat{n} \quad (4.16)$$

where  $\Delta \vec{E} = \vec{E}_i + \vec{E}_r - \vec{E}_t$  and  $\Delta \vec{D} = \vec{D}_i + \vec{D}_r - \vec{D}_t$  have been used along with (4.15) and  $\vec{D} = \epsilon \vec{E}$ .

It is now necessary to determine the field quantities inside the integration in (4.14). The quantity  $\Delta \vec{E} \cdot \hat{n}$  can be reduced to the following form through the use of (4.15);

$$\Delta \vec{E} \cdot \hat{n} = -\sqrt{\frac{\mu_o}{\epsilon_o}} H_o \frac{T_v}{\sqrt{\epsilon_r}} (\epsilon_r - 1) \exp(-j \vec{k}_i \cdot \vec{r}_\perp) (\hat{k}_t \times \hat{e}_h) \cdot \hat{n} \quad (4.17)$$

while (4.16) simplifies  $\vec{D} \cdot \hat{n}$  to

$$\vec{D} \cdot \hat{n} = -\sqrt{\mu_o \epsilon_o} H_o T_v \sqrt{\epsilon_r} \exp(-j \vec{k}_i \cdot \vec{r}_\perp) (\hat{k}_t \times \hat{e}_h) \cdot \hat{n} \quad (4.18)$$

so

$$(\Delta \vec{E} \cdot \hat{n})(\vec{D} \cdot \hat{n}) = \mu_o H_o^2 T_v (\epsilon_r - 1) \exp(-j 2 \vec{k}_i \cdot \vec{r}_\perp) [(\hat{k}_t \times \hat{e}_h) \cdot \hat{n}]^2 \quad (4.19)$$

Through similar manipulations,

$$\Delta \vec{D} \cdot \hat{\tau} = -\sqrt{\mu_o \epsilon_o} H_o \frac{T_v}{\sqrt{\epsilon_r}} (1 - \epsilon_r) \exp(-j \vec{k}_i \cdot \vec{r}_\perp) (\hat{k}_t \times \hat{e}_h) \cdot \hat{\tau} \quad (4.20)$$

and

$$\vec{E} \cdot \hat{\tau} = -\sqrt{\frac{\mu_o}{\epsilon_o}} H_o \frac{T_v}{\sqrt{\epsilon_r}} \exp(-j \vec{k}_i \cdot \vec{r}_\perp) (\hat{k}_t \times \hat{e}_h) \cdot \hat{\tau} \quad (4.21)$$

80

$$(\Delta \vec{D} \cdot \hat{r})(\vec{E}' \cdot \hat{r}) = \mu_0 H_0^2 \frac{T_v^2}{\epsilon_r} (1 - \epsilon_r) \exp(-j \vec{k}_1 \cdot \vec{r}_\perp) [(\hat{k}_t \times \hat{e}_h) \cdot \hat{r}]^2 \quad (4.22)$$

Combining (4.19) and (4.22) and completing the unit vector operations yields

$$(\Delta \vec{E} \cdot \hat{n})(\vec{D}' \cdot \hat{n}) - (\Delta \vec{D} \cdot \hat{r})(\vec{E}' \cdot \hat{r}) = \mu_0 H_0^2 T_v^2 \frac{(\epsilon_r - 1)}{\epsilon_r^2} [\epsilon_r + (\epsilon_r - 1) \sin^2 \theta] \exp(-j 2 \vec{k}_1 \cdot \vec{r}_\perp) \quad (4.23)$$

where

$$T_v = \frac{2 \epsilon_r \cos \theta}{\epsilon_r \cos \theta + \sqrt{\epsilon_r - \sin^2 \theta}}$$

Substituting this result in (4.14) and recognizing that  $E_0 = \sqrt{\frac{\mu_0}{\epsilon_0}} H_0$  and  $\hat{e}_v = -\hat{k}_1 \times \hat{e}_h$ , the final result is obtained

$$\delta \vec{E} \cdot \hat{e}_v = \frac{k_0^2 \exp(-j k_0 R)}{4 \pi R} \sqrt{\frac{\mu_0}{\epsilon_0}} H_0 T_v^2 \frac{(\epsilon_r - 1)}{\epsilon_r^2} [\epsilon_r + (\epsilon_r - 1) \sin^2 \theta] \iint \exp(-j 2 \vec{k}_1 \cdot \vec{r}_\perp) \zeta_s dx dy \quad (4.24)$$

Essentially the same remarks apply to the vertically polarized scattered field as for the horizontal case. In addition, it should be noted that if (4.11) and (4.24) are converted to  $\sigma^\circ$  or the scattering cross section per unit area according to

$$\sigma^\circ(\theta, \phi) = \lim_{R \rightarrow \infty} \lim_{A \rightarrow \infty} \left\{ \frac{4 \pi R^2}{A} \frac{\langle |\delta \vec{E}|^2 \rangle}{E_0^2} \right\}$$

where  $A$  is the illuminated area, the result is identical to the result obtained by Peake using the Rayleigh-Rice approach [1].

### 4.3 Bistatic Scattering From A Dielectric Surface With Small Roughness

For bistatic scattering the unit vectors specifying the directions of incidence of the unprimed and primed fields are given by (see Figure 4-1)

$$\begin{aligned}\hat{k}_i &= -\sin \theta_i \cos \phi_i \hat{x} - \sin \theta_i \sin \phi_i \hat{y} - \cos \theta_i \hat{z} \\ \hat{k}'_i &= -\sin \theta_s \cos \phi_s \hat{x} - \sin \theta_s \sin \phi_s \hat{y} - \cos \theta_s \hat{z}\end{aligned}\quad (4.25)$$

and  $\vec{k}_i = k_o \hat{k}_i$ ,  $\vec{k}'_i = k_o \hat{k}'_i$ . The unit vectors specifying the directions of horizontal and vertical polarizations for the unprimed and unprimed fields are as follows;

$$\begin{aligned}\hat{e}_h &= -\sin \theta_i \hat{x} + \cos \phi_i \hat{y} \\ \hat{e}'_h &= -\sin \phi_s \hat{x} + \cos \phi_s \hat{y} \\ \hat{e}_v &= -\cos \theta_i \cos \phi_i \hat{x} - \cos \theta_i \sin \phi_i \hat{y} + \sin \theta_i \hat{z} \\ \hat{e}'_v &= -\cos \theta_s \cos \phi_s \hat{x} - \cos \theta_s \sin \phi_s \hat{y} + \sin \theta_s \hat{z}\end{aligned}\quad (4.26)$$

The normal to the unperturbed surface is  $\hat{n} = \hat{z}$  while the tangents to the surface for vertical polarizations are given by

$$\hat{\tau} = \hat{n} \times \hat{e}_h \quad \hat{\tau}' = \hat{n} \times \hat{e}'_h \quad (4.27)$$

Equations (4.25)-(4.27) describe the basic quantities that will be required in this section.

#### 4.3.1 Horizontal Polarization

Since  $\Delta \vec{B}$  and  $\Delta \vec{H}$  are zero, because there is no change in  $\mu_r$  across  $S_o$  and the conductivity is finite, (4.3) becomes

$$\delta \vec{E} \cdot \hat{e}_h' = \frac{k_o^2 \exp(-j k_o R)}{4\pi R E_o \epsilon_o} \int_S [\Delta \vec{E} \cdot \vec{D}' - \Delta \vec{D} \cdot \vec{E}'] \zeta_s d S_o \quad (4.28)$$

Furthermore,  $\Delta \vec{E}$  is also zero across  $S_0$  because  $\vec{E}$  is tangential to  $S_0$ . Thus, (4.28) becomes

$$\delta^1 \vec{E} \cdot \hat{e}_h' = - \frac{k_o^2 \exp(-j k_o R)}{4\pi R E_o \epsilon_o} \int_S [\Delta \vec{D} \cdot \vec{E}'] \zeta_s dS_0 \quad (4.29)$$

On the surface  $S_0$ , the incident, reflected, and transmitted electric fields (unprimed and primed) are as follows;

$$\begin{aligned} \vec{E}_i &= E_o \exp(-j \vec{k}_i \cdot \vec{r}_\perp) \hat{e}_h & \vec{E}_i' &= E_o \exp(-j \vec{k}_i' \cdot \vec{r}_\perp) \hat{e}_h' \\ \vec{E}_r &= E_o R_h \exp(-j \vec{k}_r \cdot \vec{r}_\perp) \hat{e}_h & \vec{E}_r' &= E_o R_h' \exp(-j \vec{k}_r' \cdot \vec{r}_\perp) \hat{e}_h' \\ \vec{E}_t &= E_o T_h \exp(-j \vec{k}_t \cdot \vec{r}_\perp) \hat{e}_h & \vec{E}_t' &= E_o T_h' \exp(-j \vec{k}_t' \cdot \vec{r}_\perp) \hat{e}_h' \end{aligned} \quad (4.30)$$

where also on the surface  $S_0$ ,

$$\vec{k}_i \cdot \vec{r}_\perp = \vec{k}_r \cdot \vec{r}_\perp = \vec{k}_t \cdot \vec{r}_\perp \quad \vec{k}_i' \cdot \vec{r}_\perp = \vec{k}_r' \cdot \vec{r}_\perp = \vec{k}_t' \cdot \vec{r}_\perp \quad (4.31)$$

and the same notation as introduced earlier has been continued. The fields  $\Delta \vec{D}$  and  $\vec{E}'$  on  $S_0$  are as follows;

$$\begin{aligned} \Delta \vec{D} &= \epsilon_o E_o (1 + R_h - \epsilon_r T_h) \exp(-j \vec{k}_i \cdot \vec{r}_\perp) \hat{e}_h \\ \vec{E}' &= E_o (1 + R_h') \exp(-j \vec{k}_i' \cdot \vec{r}_\perp) \hat{e}_h' \end{aligned}$$

Using the fact that  $1 + R_h = T_h$ , the product  $\Delta \vec{D} \cdot \vec{E}'$  becomes

$$\Delta \vec{D} \cdot \vec{E}' = \epsilon_o E_o^2 (1 + R_h) (1 + R_h') (1 - \epsilon_r) (\hat{e}_h \cdot \hat{e}_h') \exp \left[ -j (\vec{k}_i + \vec{k}_i') \cdot \vec{r}_\perp \right]$$

and substituting this result in (4.29) yields

$$\delta^1 \vec{E} \cdot \hat{e}_h' = \frac{k_o^2 \exp(-j k_o R)}{4\pi R} E_o (1 + R_h) (1 + R_h') (\epsilon_r - 1) (\hat{e}_h \cdot \hat{e}_h') \iint \exp \left[ -j (\vec{k}_i + \vec{k}_i') \cdot \vec{r}_\perp \right] \zeta_s dx dy \quad (4.32)$$

This result can be easily translated into the angles  $(\theta_1, \phi_1)$  and  $(\theta_s, \phi_s)$  by the use of (4.25) and

$$\hat{e}_h \cdot \hat{e}_h' = \cos(\phi_1 - \phi_s)$$

along with

$$1 + R_h = \frac{2 \cos \theta_1}{\cos \theta_1 + \sqrt{\epsilon_r - \sin^2 \theta_1}} \quad 1 + R_h' = \frac{2 \cos \theta_s}{\cos \theta_s + \sqrt{\epsilon_r - \sin^2 \theta_s}}$$

For ease of comparison, it should be noted that most results similar to (4.32) express the direction of scattering as  $\hat{k}_s$  which, in the above notation, is  $-\hat{k}_1'$ . Equation (4.32) yields  $\delta^1 E_{hh'}$ . For cross polarized sampling of the scattered field, the problem becomes somewhat more involved and it will be discussed in Section 4.3.3. It should be noted that when  $\phi_s = \phi_1$  (backscattering), (4.32) reduces to the result obtained in Section 4.2.1.

#### 4.3.2 Vertical Polarization

Since  $\hat{n} \cdot \vec{E}$  and  $\hat{t} \cdot \vec{D}$  are discontinuous across the unperturbed surface, (4.3) reduces to

$$\delta^1 \vec{E} \cdot \hat{e}_v' = \frac{k_o^2 \exp(-jk_o R)}{4\pi R \epsilon_o \epsilon_o} \int_{S_o} [(\Delta \vec{E} \cdot \hat{n})(\vec{D}' \cdot \hat{n}) - (\Delta \vec{D} \cdot \hat{t})(\vec{E}' \cdot \hat{t}')(\hat{t} \cdot \hat{t}')] \zeta_s dS_o \quad (4.33)$$

where the scalar product  $\hat{t} \cdot \hat{t}'$  must be included because the unit vectors  $\hat{t}$  and  $\hat{t}'$  are not necessarily parallel, e.g. see (4.27). The incident, reflected, and transmitted unprimed and primed magnetic field quantities are given by

$$\begin{aligned} \vec{H}_1 &= H_o \exp(-j \vec{k}_1 \cdot \vec{r}_\perp) \hat{e}_h & \vec{H}_1' &= H_o \exp(-j \vec{k}_1' \cdot \vec{r}_\perp) \hat{e}_h' \\ \vec{H}_r &= H_o R_v \exp(-j \vec{k}_r \cdot \vec{r}_\perp) \hat{e}_h & \vec{H}_r' &= H_o R_v' \exp(-j \vec{k}_r' \cdot \vec{r}_\perp) \hat{e}_h' \\ \vec{H}_t &= H_o T_v \exp(-j \vec{k}_t \cdot \vec{r}_\perp) \hat{e}_h & \vec{H}_t' &= H_o T_v' \exp(-j \vec{k}_t' \cdot \vec{r}_\perp) \hat{e}_h' \end{aligned} \quad (4.34)$$

while the corresponding electric fields are

$$\begin{aligned}
 \vec{E}_1 &= -\sqrt{\frac{\mu_0}{\epsilon_0}} \hat{k}_1 \times \vec{H}_1 & \vec{E}'_1 &= -\sqrt{\frac{\mu_0}{\epsilon_0}} \hat{k}'_1 \times \vec{H}'_1 \\
 \vec{E}_r &= -\sqrt{\frac{\mu_0}{\epsilon_0}} \hat{k}_r \times \vec{H}_r & \vec{E}'_r &= -\sqrt{\frac{\mu_0}{\epsilon_0}} \hat{k}'_r \times \vec{H}'_r \\
 \vec{E}_t &= -\sqrt{\frac{\mu_0}{\epsilon_0 \epsilon_r}} \hat{k}_t \times \vec{H}_t & \vec{E}'_t &= -\sqrt{\frac{\mu_0}{\epsilon_0 \epsilon_r}} \hat{k}'_t \times \vec{H}'_t
 \end{aligned} \tag{4.35}$$

and  $\vec{D} = \epsilon \vec{E}$ ,  $\vec{D}' = \epsilon \vec{E}'$ . The same notation introduced in Section 4.3.2 is continued here. From the boundary condition that the tangential component of the electric field be continuous across  $S_0$ , i.e.  $\Delta \vec{E} \cdot \hat{\tau} = 0$  and  $\Delta \vec{E}' \cdot \hat{\tau}' = 0$ , the following relationships result;

$$\begin{aligned}
 (\hat{k}_1 \times \hat{e}_h) \cdot \hat{\tau} + R_h (\hat{k}_r \times \hat{e}_h) \cdot \hat{\tau} &= \frac{T_v}{\sqrt{\epsilon_r}} (\hat{k}_t \times \hat{e}_h) \cdot \hat{\tau} \\
 (\hat{k}'_1 \times \hat{e}'_h) \cdot \hat{\tau}' + R'_h (\hat{k}'_r \times \hat{e}'_h) \cdot \hat{\tau}' &= \frac{T'_v}{\sqrt{\epsilon_r}} (\hat{k}'_t \times \hat{e}'_h) \cdot \hat{\tau}'
 \end{aligned} \tag{4.36}$$

Similarly from the continuity of the normal component of the  $\vec{D}$ -field across  $S_0$ , i.e.  $\Delta \vec{D} \cdot \hat{n} = 0$  and  $\Delta \vec{D}' \cdot \hat{n} = 0$ , there results

$$\begin{aligned}
 (\hat{k}_1 \times \hat{e}_h) \cdot \hat{n} + R_v (\hat{k}_r \times \hat{e}_h) \cdot \hat{n} &= \sqrt{\epsilon_r} T_v (\hat{k}_t \times \hat{e}_h) \cdot \hat{n} \\
 (\hat{k}'_1 \times \hat{e}'_h) \cdot \hat{n} + R'_v (\hat{k}'_r \times \hat{e}'_h) \cdot \hat{n} &= \sqrt{\epsilon_r} T'_v (\hat{k}'_t \times \hat{e}'_h) \cdot \hat{n}
 \end{aligned} \tag{4.37}$$

Using (4.37) to simplify the expressions for  $\Delta \vec{E} \cdot \hat{n}$  and  $\Delta \vec{E}' \cdot \hat{n}$  yields

$$\Delta \vec{E} \cdot \hat{n} = - \sqrt{\frac{\mu_0}{\epsilon_0}} H_0 \frac{T_v}{\sqrt{\epsilon_r}} (\epsilon_r - 1) \exp(-j \vec{k}_i \cdot \vec{r}_\perp) (\hat{k}_t \times \hat{e}_h) \cdot \hat{n} \quad (4.38)$$

and

$$\vec{D}' \cdot \hat{n} = - \sqrt{\mu_0 \epsilon_0} H_0 \sqrt{\epsilon_r} T_v' \exp(-j \vec{k}_i' \cdot \vec{r}_\perp) (\hat{k}_t' \times \hat{e}_h') \cdot \hat{n} \quad (4.39)$$

In a similar fashion, (4.36) is used to simplify the expressions for  $\Delta \vec{D} \cdot \hat{\tau}$  and  $\vec{E}' \cdot \hat{\tau}'$  with the following result;

$$\Delta \vec{D} \cdot \hat{\tau} = \sqrt{\mu_0 \epsilon_0} H_0 \frac{T_v}{\sqrt{\epsilon_r}} \exp(-j \vec{k}_i \cdot \vec{r}_\perp) (\hat{k}_t \times \hat{e}_h) \cdot \hat{\tau} \quad (4.40)$$

and

$$\vec{E}' \cdot \hat{\tau}' = - \sqrt{\frac{\mu_0}{\epsilon_0}} H_0 \frac{T_v'}{\sqrt{\epsilon_r}} \exp(-j \vec{k}_i' \cdot \vec{r}_\perp) (\hat{k}_t' \times \hat{e}_h') \cdot \hat{\tau}' \quad (4.41)$$

Substituting (4.38) - (4.41) in (4.33), noting that  $\hat{\tau} \cdot \hat{\tau}' = \cos(\phi_i - \phi_s)$ , and simplifying the unit vector operations yields the following result for  $\delta \vec{E} \cdot \hat{e}_v'$ ;

$$\begin{aligned} \delta \vec{E} \cdot \hat{e}_v' &= \sqrt{\frac{\mu_0}{\epsilon_0}} H_0 \frac{\exp(-jk_o R)}{4\pi R} T_v T_v' \frac{(\epsilon_r - 1)}{\epsilon_r^2} \left\{ \epsilon_r \sin \theta_i \sin \theta_s + \sqrt{(\epsilon_r - \sin^2 \theta_i)(\epsilon_r - \sin^2 \theta_s)} \right. \\ &\quad \left. \cdot \cos(\phi_i - \phi_s) \right\} \iiint \exp[-j(\vec{k}_i + \vec{k}_i') \cdot \vec{r}_\perp] \zeta_s dx dy \quad (4.42) \end{aligned}$$

where  $E_0 = H_0 \sqrt{\mu_0 / \epsilon_0}$  and

$$T_v = 1 + R_v = \frac{2 \epsilon_r \cos \theta_i}{\epsilon_r \cos \theta_i + \sqrt{\epsilon_r - \sin^2 \theta_i}}$$

and  $T_v' = T_v(\theta_i \rightarrow \theta_s)$ . Equation (4.42) is  $\delta^1 E_{vv'}$ , and it is easily shown to reduce to the result for backscattering in Section 4.2.2. when  $\phi_i = \phi_s$  and  $\theta_i = \theta_s$ . Once again it should be emphasized that the most difficult part of obtaining (4.42) is evaluating the terms  $(\hat{k}_t \times \hat{e}_h) \cdot \hat{t}$  and  $(\hat{k}_t' \times \hat{e}_h') \cdot \hat{t}'$  in (4.40) and (4.41). As noted previously this is a consequence of the fact that the difficult analysis was finished once (4.3) was derived and the actual evaluation of (4.3) is very straightforward. Finally, comparing the  $\sigma^\circ$  values resulting from (4.32) and (4.42) with the corresponding results obtained from the Rayleigh-Rice theory [10] shows complete agreement.

#### 4.3.3 Cross Polarization

As shown in Sections 4.2.1 and 4.2.2, depolarization for scattering by small scale roughness is a second order effect in the plane of incidence. If, however, the scattered field outside of the plane of incidence is computed, it will be found to have a nonzero cross polarized component. This result is simply a consequence of the fact that the unit vectors  $\hat{e}_h'$  and  $\hat{e}_v'$  are not fixed with respect to the surface-centered coordinate system and they change their directions as the observation point moves out of the plane of incidence. This, of course, is a purely geometrical effect and it has nothing to do with any change in the basic scattering mechanism.

The derivation of the results follows essentially the same pattern as set forth in the previous sections. There is one point that should be noted because it simplifies the algebra somewhat. For the case of the incident field horizontally polarized ( $\hat{e}_h$ ) and the scattered field vertically polarized ( $\hat{e}_v'$ ), the unprimed field quantities should be obtained from

$$\vec{E}_i = E_0 \exp(-j \vec{k}_i \cdot \vec{r}_\perp) \hat{e}_h \text{ while the primed fields should be obtained from } \\ \vec{H}_i' = H_0 \exp(-j \vec{k}_i' \cdot \vec{r}_\perp) \hat{e}_h' . \text{ For the incident field vertically polarized } (\hat{e}_v)$$

and the scattered field horizontally polarized ( $\hat{e}_h'$ ), the unprimed fields are obtained from  $\vec{H}_1 = H_0 \exp(-j \vec{k}_1 \cdot \vec{r}_\perp) \hat{e}_h$  while the primed fields are to be derived from  $\vec{E}_1' = E_0 \exp(-j \vec{k}_1' \cdot \vec{r}_\perp) \hat{e}_h'$ . This approach is consistent with the technique of obtaining all field quantities from the horizontal ( $\hat{e}_h$  or  $\hat{e}_h'$ ) field for planar surface reflection.

With  $E_0 = H_0 \sqrt{\mu_0 / \epsilon_0}$ , the following expressions for  $\delta^1 E_{hv'}$  and  $\delta^1 E_{vh'}$  result;

$$\delta^1 E_{hv'} = \delta^1 \vec{E} \cdot \hat{e}_v' = \frac{k_o^2 \exp(-jk_o R)}{\pi R} E_0 \left\{ \frac{\cos \theta_i \cos \theta_s \sin(\phi_s - \phi_i) (\epsilon_r - 1) \sqrt{\epsilon_r - \sin^2 \theta_s}}{(\cos \theta_i + \sqrt{\epsilon_r - \sin^2 \theta_i}) (\epsilon_r \cos \theta_s + \sqrt{\epsilon_r - \sin^2 \theta_s})} \right\} \\ \cdot \iint \exp[-j(\vec{k}_i + \vec{k}_i') \cdot \vec{r}_\perp] \zeta_s dx dy \quad (4.43)$$

$$\delta^1 E_{vh'} = \delta^1 \vec{E} \cdot \hat{e}_h' = \frac{k_o^2 \exp(-jk_o R)}{\pi R} \sqrt{\frac{\mu_o}{\epsilon_o}} H_0 \left\{ \frac{\cos \theta_i \cos \theta_s \sin(\phi_s - \phi_i) (\epsilon_r - 1) \sqrt{\epsilon_r - \sin^2 \theta_i}}{(\cos \theta_s + \sqrt{\epsilon_r - \sin^2 \theta_s}) (\epsilon_r \cos \theta_i + \sqrt{\epsilon_r - \sin^2 \theta_i})} \right\} \\ \cdot \iint \exp[-j(\vec{k}_i + \vec{k}_i') \cdot \vec{r}_\perp] \zeta_s dx dy \quad (4.44)$$

where, in summary, the angles are defined in Figure 4.2,  $\vec{r}_\perp = x\hat{x} + y\hat{y}$ , and  $\vec{k}_i$  and  $\vec{k}_i'$  are defined as  $k_o \hat{k}_i$  and  $k_o \hat{k}_i'$ , respectively, where  $\hat{k}_i$  and  $\hat{k}_i'$  are given in (4.25).

When comparing (4.43) and (4.44) with the cross polarized scattered fields resulting from the Rayleigh-Rice approach [10],  $\phi_i$  should be set equal to  $\pi$ . The expression for  $\delta^1 E_{vh'}$  agrees with the results in [10, pg. 706]. The expression for  $\delta^1 E_{hv'}$  is, however, the negative of the  $\alpha_{hv}$  coefficient in [10, pg. 706, eqn. 9.1-69]. Normally this difference is not important because

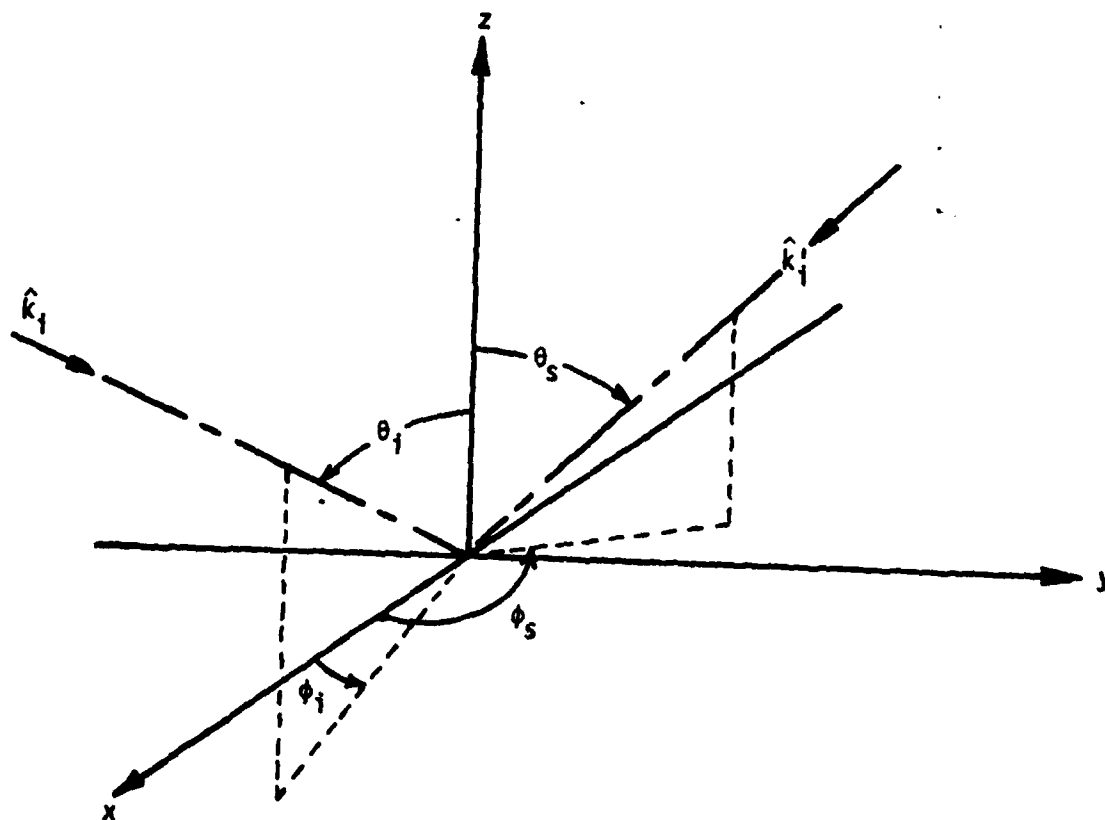


Figure 4-2. Geometry for bistatic scattering from a randomly rough surface having only small scale roughness  $\zeta_R$ .

$\delta^1 E_{hv}$ , is squared and then averaged to find the incoherent power. However, if one is dealing with circular polarization the sign does become critical. To resolve this issue, a special case can be constructed whereby  $\alpha_{hv}$  should agree with  $\alpha_{vv}$  or  $\delta^1 E_{hv} = \delta^1 E_{vv}$ . This special case involves taking  $\phi_i = \pi$  and  $\phi_s = 0$  and  $\theta_s = 0$  in the expression for  $\alpha_{vv}$  or  $\delta^1 E_{vv}$ , and comparing this result with  $\alpha_{hv}$  and  $\delta^1 E_{hv}$ , for  $\phi_i = \pi$ ,  $\phi_s = \pi/2$ , and  $\theta_s = 0$ . In this special case both  $\delta^1 E_{vv}$ , and  $\delta^1 E_{hv}$ , should be polarized in the  $-\hat{x}$ -direction. Comparing (4.42) and (4.43) for this special case shows that indeed  $\delta^1 E_{vv} = \delta^1 E_{hv}$ . However, evaluating  $\alpha_{vv}$  and  $\alpha_{hv}$  from [10] results in  $\alpha_{vv} = -\alpha_{hv}$ ; consequently, there does appear to be a sign error in the expression for  $\alpha_{hv}$  and (4.43) is correct.

This section completes the development for scattering from a dielectric surface having only a small scale roughness. Once again it should be emphasized that the purposes of Sections 4.2 and 4.3 are (1) to check the Burrows perturbation approach against the conventional Rayleigh-Rice results and (2) to illustrate the actual mechanics of evaluating the Burrows expression for the first order perturbation field. Hopefully, this latter purpose, if achieved, should considerably simplify the transition to the composite surface case.

#### 4.4 Bistatic Scattering From A Dielectric Surface With Composite Roughness

For small scale roughness superposed on a planar surface, the Burrows perturbation formula (4.3) is particularly easy to evaluate. This results from the fact that one deals with the fields on an infinite planar surface and, for such a surface, the fields are easily described and related through the Fresnel coefficients, Snell's law, and the equality of the angles of incidence and reflection. For a composite surface, the unperturbed surface is not planar but it is assumed to be very gently undulating. More specifically, the unperturbed surface is actually defined such that it contains no spatial frequency

components which are smaller than  $\gamma k_0$ , where  $\gamma$  is a constant which is greater than unity. Of course, it is desirable to have  $\gamma$  as large as possible but this is not always practical since the small scale height must satisfy  $4k_0^2 \zeta_s^2 \ll 1$  [6]. However, if  $\gamma$  can be made sufficiently large then the scattering from the unperturbed surface can be treated using physical optics.

Physical optics assumes that the surface may be considered to be locally planar and the fields on the surface can be accurately approximated using Fresnel theory. This approach is recognized to be essentially the same as the small scale roughness on a planar surface problem. The one important difference is that for the gently undulating unperturbed surface, the local normal is no longer entirely z-directed and, in fact, depends upon the slopes of the large scale surface. This means that one must construct a local coordinate system on the undulating unperturbed surface and compute the surface fields required in (4.3) in terms of this system. This must be done for both the unprimed and primed fields because they have different angles and directions of incidence for the general bistatic case.

For the unprimed fields, the important unit vectors are  $\hat{k}_i$  and  $\hat{n}_l$  which is the normal to the large scale or unperturbed surface. These two quantities are important because they form the local plane of incidence. One next constructs unit vectors  $\hat{e}_{lh}$  and  $\hat{e}_{lv}$  which are orthogonal and parallel, respectively, to  $\hat{k}_i$  and  $\hat{n}_l$ . These unit vectors are also horizontally and vertically polarized, respectively, with respect to the local plane of incidence. Any arbitrarily polarized unprimed incident field can now be decomposed into components parallel to  $\hat{e}_{lh}$  and  $\hat{e}_{lv}$  since the incident field must be transverse to  $\hat{k}_i$ . The unprimed field quantities required in (4.3) can then be computed as in the previous sections. The exact same construction of  $\hat{e}'_{lh}$  and  $\hat{e}'_{lv}$  and the decomposition of the primed incident field must be performed

in order to compute the primed fields required in (4.3). Fortunately, this is easily accomplished by simply changing  $\theta_i$  to  $\theta_s$  and  $\phi_i$  to  $\phi_s$  in the unprimed quantities.

Before getting into the actual details, there are a few other points that should be noted. All of the above noted manipulations are going to lead to the following changes in  $\delta^1 \vec{E}$  obtained in equation (16) of [6]. First, the factor  $\Gamma_{pp'}$  is going to depend on  $\epsilon_r$ , the angles and directions of incidence and scattering  $(\theta_i, \phi_i, \theta_s, \phi_s)$ , and the slopes of the large scale or unperturbed surface  $(\zeta_{lx}, \zeta_{ly})$ . The only other change is that the exponential inside the surface integral will become  $\exp[-j(\vec{k}_i + \vec{k}_i') \cdot \vec{r}_l]$  where  $\vec{r}_l = x\hat{x} + y\hat{y} + \zeta_l \hat{z}$  because of the generalization to bistatic scattering. Except for correcting [6] to properly include shadowing, as detailed in Section 2, all other aspects of the solution presented in [6] remain the same. Combining  $\delta^1 \vec{E}$  from this analysis with Sancer's result [11] for essentially  $\delta^0 \vec{E}$  yields the total scattered field. Furthermore, it should be expected that for backscattering the dielectric nature of the surface should have an almost negligible effect upon the wavenumber at which the surface height spectrum is partitioned into large and small scale sub-spectra. Finally, because there is no discontinuity in magnetic properties across the unperturbed surface and the conductivity is assumed to be finite,  $\Delta \vec{B}$  and  $\Delta \vec{H}$  in (4.3) will be zero. This fact holds true regardless of any tilting of the locally planar surface.

The first task at hand is to construct  $\hat{e}_{lh}$  and  $\hat{e}_{lv}$ . Since  $\hat{e}_{lh}$  is orthogonal to both  $\hat{k}_i$  and  $\hat{n}_l$ , it is given by

$$\hat{e}_{lh} = \frac{\hat{k}_i \times \hat{n}_l}{|\hat{k}_i \times \hat{n}_l|} \quad (4.45)$$

where  $\hat{k}_i = k_{ix} \hat{x} + k_{iy} \hat{y} + k_{iz} \hat{z}$  and the  $k_{iq}$ ,  $q = x, y$  and  $z$ , are obvious from (4.25). The normal to the large scale surface is given by

$$\hat{n}_\ell = \frac{-\zeta_{\ell x} \hat{x} - \zeta_{\ell y} \hat{y} + \hat{z}}{\sqrt{1 + \zeta_{\ell x}^2 + \zeta_{\ell y}^2}} = n_{\ell x} \hat{x} + n_{\ell y} \hat{y} + n_{\ell z} \hat{z} \quad (4.46)$$

Expanding the cross product in (4.45) yields

$$\hat{e}_{\ell h} = h_{\ell x} \hat{x} + h_{\ell y} \hat{y} + h_{\ell z} \hat{z} \quad (4.47)$$

where

$$h_{\ell x} = \frac{(k_{iy} n_{\ell z} - k_{iz} n_{\ell y})}{|\hat{k}_i \times \hat{n}_\ell|} \quad h_{\ell y} = \frac{(k_{iz} n_{\ell x} - k_{ix} n_{\ell z})}{|\hat{k}_i \times \hat{n}_\ell|}$$

$$h_{\ell z} = \frac{(k_{ix} n_{\ell y} - k_{iy} n_{\ell x})}{|\hat{k}_i \times \hat{n}_\ell|}$$

and  $\hat{e}_{\ell h}$  is completely determined. For the unit vector  $\hat{e}_{\ell v}$ , things are a bit more involved because it must be in the plane formed by  $\hat{k}_i$  and  $\hat{n}_\ell$  and also orthogonal to  $\hat{e}_{\ell h}$ . For the reflected and transmitted fields  $\hat{k}_i$  goes to  $\hat{k}_r$  and  $\hat{k}_t$ . This will not change the direction of  $\hat{e}_{\ell h}$  because  $\hat{k}_i, \hat{k}_r$  and  $\hat{k}_t$  are all coplanar. This will, however, alter the direction of  $\hat{e}_{\ell v}$ ; this is easily understood by noting that  $\hat{k}_q, \hat{e}_{\ell h}$ , and  $\hat{e}_{\ell v}$  form a mutually orthogonal triad of unit vectors. Thus, if  $\hat{e}_{\ell h}$  does not change direction but  $\hat{k}_q$  does then  $\hat{e}_{\ell v}$  must necessarily change direction. What this means is that we must find a new  $\hat{e}_{\ell v}$  for each value of  $\hat{k}_q$ . This is easily done by the following equality;

$$\hat{e}_{\ell v}^q = \hat{e}_{\ell h} \times \hat{k}_q \quad (4.48)$$

where  $q = i, r$ , and  $t$ . Note that it is not necessary to divide the rhs of (4.48) by the magnitude because it is unity, i.e.  $\hat{e}_{\ell h}$  and  $\hat{k}_q$  are mutually orthogonal by (4.45). The unit vector  $\hat{e}_{\ell v}^q$  may also be written as

$$\hat{e}_{lv}^q = v_{lx}^q \hat{x} + v_{ly}^q \hat{y} + v_{lz}^q \hat{z} \quad (4.49)$$

where

$$v_{lx}^q = -(k_{qy} h_{lz} - k_{qz} h_{ly}) \quad v_{ly}^q = -(k_{qx} h_{lz} - k_{qz} h_{lx})$$

$$v_{lz}^q = -(k_{qx} h_{ly} - k_{qy} h_{lx})$$

and  $\hat{e}_{lv}^q$  is completely determined for  $q = i, r$ , and  $t$ . For the primed fields,  $\hat{e}_{lh}^q$  and  $\hat{e}_{lv}^q$  are obtained by merely replacing  $\vec{k}_q$  by  $\vec{k}_q'$ ,  $q = i, r$ , and  $t$ , in the expressions for  $\hat{e}_{lh}$  and  $\hat{e}_{lv}$ .

The incident, reflected, and transmitted unprimed fields on the unperturbed surface will now be decomposed into locally horizontal and vertical components. If the incident field is of the form  $\vec{E}_i = E_0 \exp(-j \vec{k}_i \cdot \vec{r}_\perp) \hat{e}_a$  on the unperturbed surface where  $\hat{e}_a$  is its polarization direction then  $\vec{E}_i$ ,  $\vec{E}_r$  and  $\vec{E}_t$  can be written as follows;

$$\begin{aligned} \vec{E}_i &= E_h^i \hat{e}_{lh} + E_v^i \hat{e}_{lv}^i \\ \vec{E}_r &= E_h^r \hat{e}_{lh} + E_v^r \hat{e}_{lv}^r \\ \vec{E}_t &= E_h^t \hat{e}_{lh} + E_v^t \hat{e}_{lv}^t \end{aligned} \quad (4.50)$$

where

$$\begin{aligned} E_h^q &= E_0 \exp(-j \vec{k}_q \cdot \vec{r}_\perp) (\hat{e}_a \cdot \hat{e}_{lh}) \\ E_v^q &= E_0 \exp(-j \vec{k}_q \cdot \vec{r}_\perp) (\hat{e}_a \cdot \hat{e}_{lv}^q) \end{aligned} \quad (4.51)$$

and  $q = i, r, t$ . The corresponding magnetic fields are given by

$$\vec{H}_q = \sqrt{\frac{\epsilon_0}{\mu_0}} \hat{k}_q \times \vec{E}_q \frac{\sqrt{\epsilon_r}}{\delta_{qt}} \quad (4.52)$$

where  $\delta_{qt} = \sqrt{\epsilon_r}$  for  $q = i$  and  $r$ , and  $\delta_{tt} = 1$ . Expanding (4.52) yields

$$\vec{H}_i = \sqrt{\frac{\epsilon_o}{\mu_o}} \left( -E_h^i \hat{e}_{lv}^i + E_v^i \hat{e}_{lh}^i \right)$$

$$\vec{H}_r = \sqrt{\frac{\epsilon_o}{\mu_o}} \left( -E_h^r \hat{e}_{lv}^r + E_v^r \hat{e}_{lh}^r \right)$$

$$\vec{H}_t = \sqrt{\frac{\epsilon_o \epsilon_r}{\mu_o}} \left( -E_h^t \hat{e}_{lv}^t + E_v^t \hat{e}_{lh}^t \right)$$

From Fresnel theory, the  $\hat{e}_{lh}$ -component of  $\vec{H}_r$  is equal to  $R_{v\ell}$  times the  $\hat{e}_{lh}$ -component of  $\vec{H}_i$ , so

$$E_v^r = R_{v\ell} E_v^i \quad (4.53)$$

Similarly, the  $\hat{e}_{lv}$ -component of  $\vec{H}_t$  is equal to  $T_{v\ell}$  times the  $\hat{e}_{lv}$ -component of  $\vec{H}_i$ , so

$$E_v^t = \frac{T_{v\ell}}{\sqrt{\epsilon_r}} E_v^i \quad (4.54)$$

Equations (4.53) and (4.54) can now be used in (4.50) to express all of the fields in terms of  $E_v^i$  and  $E_h^i$ , i.e.

$$\begin{aligned} \vec{E}_i &= E_h^i \hat{e}_{lh} + E_v^i \hat{e}_{lv} \\ \vec{E}_r &= R_{h\ell} E_h^i \hat{e}_{lh} + R_{v\ell} E_v^i \hat{e}_{lv} \\ \vec{E}_t &= T_{h\ell} E_h^i \hat{e}_{lh} + \frac{T_{v\ell}}{\sqrt{\epsilon_r}} E_v^i \hat{e}_{lv} \end{aligned} \quad (4.55)$$

\*The subscripts " $\ell$ " on  $R_v$ ,  $R_h$ ,  $T_v$ ,  $T_h$  means that the angles in the appropriate Fresnel formulas must be defined with respect to the normal to the large scale surface,  $\hat{n}_\ell$ .

where  $E_h^1$  and  $E_v^1$  are given by (4.52) with  $q=1$ . The corresponding  $\vec{D}$ -fields are;  $\vec{D}_1 = \epsilon_0 E_1$ ,  $\vec{D}_r = \epsilon_0 \vec{E}_r$ ,  $\vec{D}_t = \epsilon_0 \epsilon_r \vec{E}_t$ . The primed fields may be obtained from (4.55) and (4.51) by replacing  $\hat{k}_q$  by  $\hat{k}_q'$ ,  $\hat{e}_{lh}$  by  $\hat{e}_{lh}'$ ,  $\hat{e}_{lv}^q$  by  $\hat{e}_{lv}^{q'}$  and by changing  $\hat{e}_a$  to whatever scattered field polarization is to be sampled, say,  $\hat{e}_b$ .

The appropriate form of (4.3) is

$$\delta' \vec{E} \cdot \hat{e}_b = \frac{k_o^2 \exp(-j k_o R)}{4\pi R E_o \epsilon_o} \int_{S_o} [(\Delta \vec{E} \cdot \hat{n}_\ell) (\vec{D}' \cdot \hat{n}_\ell) - \Delta \vec{D} \cdot \vec{E}'] \epsilon_s dS_o \quad (4.56)$$

where the shadowing factor has been temporarily omitted from the integrand since it can be added at the end of the development. The  $(\Delta \vec{E} \cdot \hat{n}_\ell)$  is equal to  $(\vec{E}_1 + \vec{E}_r - \vec{E}_t) \cdot \hat{n}_\ell$  or using (4.55) and noting that  $\hat{n}_\ell \cdot \hat{e}_{lh} = 0$ ,

$$\Delta \vec{E} \cdot \hat{n}_\ell = E_v^1 \left( \hat{e}_{lv}^1 \cdot \hat{n}_\ell + R_{v_\ell} \hat{e}_{lv}^r \cdot \hat{n}_\ell - \frac{T_{v_\ell}}{\sqrt{\epsilon_r}} \hat{e}_{lv}^t \cdot \hat{n}_\ell \right) \quad (4.57)$$

(4.57) can be simplified somewhat by using the relationship that results from  $\Delta \vec{D} \cdot \hat{n} = 0$ . The final result is

$$\Delta \vec{E} \cdot \hat{n}_\ell = E_v^1 \frac{(\epsilon_r - 1)}{\sqrt{\epsilon_r}} T_{v_\ell} (\hat{e}_{lv}^t \cdot \hat{n}_\ell) \quad (4.58)$$

For  $\vec{D}' \cdot \hat{n}_\ell$ ,

$$\vec{D}' \cdot \hat{n}_\ell = E_v^1 \epsilon_o \sqrt{\epsilon_r} T_{v_\ell}' (\hat{e}_{lv}^{t'} \cdot \hat{n}_\ell) \quad (4.59)$$

so the product of (4.58) and (4.59) can be written as follows

$$(\Delta \vec{E} \cdot \hat{n}_\ell) (\vec{D}' \cdot \hat{n}_\ell) = E_o^2 \exp \left[ -j (\vec{k}_1 + \vec{k}_1') \cdot \vec{r}_\perp \right] \epsilon_o (\epsilon_r - 1) T_{v_\ell}' T_{v_\ell} (\hat{e}_{lv}^t \cdot \hat{n}_\ell) (\hat{e}_{lv}^{t'} \cdot \hat{n}_\ell) \quad (4.60)$$

It can be shown that

$$\hat{e}_{lv}^t \cdot \hat{n}_l = \frac{\sin \theta_{l1}}{\sqrt{\epsilon_r}}$$

and

$$\hat{e}_{lv}^{t'} \cdot \hat{n}_l = \frac{\sin \theta_{l1}'}{\sqrt{\epsilon_r}}$$

where

$$\sin \theta_{l1} = \sqrt{1 - (\hat{k}_1 \cdot \hat{n}_l)^2}$$

$$\sin \theta_{l1}' = \sqrt{1 - (\hat{k}_1' \cdot \hat{n}_l)^2}$$

so (4.60) becomes

$$(\Delta \vec{E} \cdot \hat{n}_l)(\vec{D}' \cdot \hat{n}_l) = E_0^2 \epsilon_0 (\epsilon_r - 1) T_{v_l}^{t'} T_{v_l} \frac{\sqrt{1 - (\hat{k}_1 \cdot \hat{n}_l)^2} \sqrt{1 - (\hat{k}_1' \cdot \hat{n}_l)^2}}{\epsilon_r} \exp[-j(\hat{k}_1 + \hat{k}_1') \cdot \vec{r}_l] \quad (4.61)$$

For the remaining term in (4.56), the important parts are  $(\Delta \vec{D})_p$  and  $(\vec{E}')_p$  where the p-subscript denotes tangential to the large scale surface, i.e. the normal component of  $\vec{D}$  is continuous across the boundary so  $\Delta \vec{D} \cdot \hat{n}_l = 0$ . The tangential components of the  $\Delta \vec{D}$ -field can be found by decomposing  $\Delta \vec{D}$  into components directed along  $\hat{e}_{lh}$  and  $\tau_l$ , where  $\tau_l = \hat{n}_l \times \hat{e}_{lh}$ , i.e.

$$(\Delta \vec{D})_p = (\Delta \vec{D} \cdot \hat{e}_{lh}) \hat{e}_{lh} + (\Delta \vec{D} \cdot \tau_l) \tau_l \quad (4.62)$$

Using

$$\Delta \vec{D} = \epsilon_0 E_h^i (1 + R_{h_l} - \epsilon_r T_{h_l}) \hat{e}_{lh} + \epsilon_0 E_v^i (\hat{e}_{lv}^i + R_{v_l} \hat{e}_{lv}^r - T_v \sqrt{\epsilon_r} \hat{e}_{lv}^t)$$

and simplifying this expression with the aid of

$$(\hat{e}_{lv}^1 \cdot \hat{t}_l) + R_{vl} (\hat{e}_{lv}^r \cdot \hat{t}_l) = \frac{T_{vl}}{\sqrt{\epsilon_r}} (\hat{e}_{lv}^t \cdot \hat{t})$$

which results from  $(\Delta \vec{E})_p = 0$  yields

$$(\Delta \vec{D})_p = -\epsilon_0 E_h^1 (1 + R_{hl}) (\epsilon_r - 1) \hat{e}_{lh} - \frac{\epsilon_0}{\sqrt{\epsilon_r}} E_v^1 T_{vl} (\epsilon_r - 1) (\hat{e}_{lv}^t \cdot \hat{t}) \quad (4.63)$$

The appropriate expression for  $(\vec{E}')_p$  is

$$(\vec{E}')_p = E_h^{1'} T_{hl}' \hat{e}_{lh}' + E_v^{1'} \frac{T_{vl}'}{\sqrt{\epsilon_r}} (\hat{e}_{lv}^{t'} \cdot \hat{t}_l') \hat{t}_l' \quad (4.64)$$

since on the unperturbed surface  $\vec{E}' = \vec{E}'_1 + \vec{E}'_r = \vec{E}'_t$ . The relationship for  $(\Delta \vec{D})_p (\vec{E}')_p$  is obtained by taking the dot product of (4.63) with (4.64). Combining this result with (4.61) and substituting into (4.56) yields the following result;

$$\delta^1 E_{ab} = \frac{E_0 k_0^2 \exp(-jk_0 R)}{\pi R} \iint \Gamma_{ab}(\zeta_{lx}, \zeta_{ly}) I(x, y) \exp[-j(\hat{k}_1 + \hat{k}_1') \cdot \vec{r}_l] \zeta_s dx dy \quad (4.65)$$

where  $\delta^1 E_{ab}$  is the scattered first order perturbation field for an incident polarization  $\hat{e}_a$  and scattered polarization  $\hat{e}_b$ ,  $I(x, y)$  is unity on the illuminated parts of the surface and zero for the shadowed parts, and

$$\begin{aligned}
\Gamma_{ab} = & \frac{(\epsilon_r - 1)}{4} \sqrt{1 + \zeta_{lx}^2 + \zeta_{ly}^2} \left\{ (\hat{e}_a \cdot \hat{e}_{lv}^1) (\hat{e}_b \cdot \hat{e}_{lv}^{1'}) \left( \frac{T_{vl} T_{vl}'}{\epsilon_r^2} \right) \left[ \epsilon_r \sin \theta_{l1} \sin \theta_{l1}' \right. \right. \\
& + \sqrt{\epsilon_r - \sin^2 \theta_{l1}} \sqrt{\epsilon_r - \sin^2 \theta_{l1}'} \left( \frac{\hat{k}_1 \cdot \hat{k}_1' - (\hat{n}_l \cdot \hat{k}_1) (\hat{n}_l \cdot \hat{k}_1')}{\sin \theta_{l1} \sin \theta_{l1}'} \right) \left. \right] + (\hat{e}_a \cdot \hat{e}_{lh}) (\hat{e}_b \cdot \hat{e}_{lh}') T_{hl} T_{hl}' \\
& \cdot \left[ \frac{\hat{k}_1 \cdot \hat{k}_1' - (\hat{n}_l \cdot \hat{k}_1) (\hat{n}_l \cdot \hat{k}_1')}{\sin \theta_{l1} \sin \theta_{l1}'} \right] + \left[ (\hat{e}_a \cdot \hat{e}_{lv}^1) (\hat{e}_b \cdot \hat{e}_{lh}') T_{hl}' \left( \frac{T_{vl}}{\epsilon_r} \right) \sqrt{\epsilon_r - \sin^2 \theta_{l1}} \right. \\
& + (\hat{e}_b \cdot \hat{e}_{lv}^{1'}) (\hat{e}_a \cdot \hat{e}_{lh}) T_{hl} \left( \frac{T_{vl}'}{\epsilon_r} \right) \sqrt{\epsilon_r - \sin^2 \theta_{l1}'} \left. \right] \left[ \frac{\hat{n}_l \cdot (\hat{k}_1 \times \hat{k}_1')}{\sin \theta_{l1} \sin \theta_{l1}'} \right] \left. \right\} \quad (4.66)
\end{aligned}$$

For convenience, the above terms are summarized below

$\hat{e}_a$  = Polarization of the incident electric field ( $\vec{E}_i = E_o^i \hat{e}_a$ )

$\hat{e}_b$  = Polarization of the scattered electric field ( $\vec{E}_s = E_o^s \hat{e}_b$ )

$$\hat{n}_l = \frac{-\zeta_{lx} \hat{x} - \zeta_{ly} \hat{y} + \hat{z}}{\sqrt{1 + \zeta_{lx}^2 + \zeta_{ly}^2}}$$

$$\vec{k}_1 = k_o \hat{k}_1 \quad ; \quad \hat{k}_1 = -\sin \theta_1 \cos \phi_1 \hat{x} - \sin \theta_1 \sin \phi_1 \hat{y} - \cos \theta_1 \hat{z}$$

$$\vec{k}_1' = k_o \hat{k}_1' \quad ; \quad \hat{k}_1' = -\sin \theta_s \cos \phi_s \hat{x} - \sin \theta_s \sin \phi_s \hat{y} - \cos \theta_s \hat{z}$$

$$\hat{e}_{lh} = \frac{\hat{k}_1 \times \hat{n}_l}{|\hat{k}_1 \times \hat{n}_l|} \quad \hat{e}_{lh}' = \frac{\hat{k}_1' \times \hat{n}_l}{|\hat{k}_1' \times \hat{n}_l|} \quad \hat{e}_{lv}^1 = \hat{e}_{lh} \times \hat{k}_1 \quad \hat{e}_{lv}^{1'} = \hat{e}_{lh}' \times \hat{k}_1'$$

$$\sin \theta_{l1} = |\hat{k}_1 \times \hat{n}_l| \quad \sin \theta_{l1}' = |\hat{k}_1' \times \hat{n}_l|$$

$$\vec{r}_l = x \hat{x} + y \hat{y} + \zeta_l \hat{z}$$

$$T_{v_l} = \frac{2\epsilon_r \cos \theta_{l1}}{\epsilon_r \cos \theta_{l1} + \sqrt{\epsilon_r - \sin^2 \theta_{l1}}}$$

$$T'_{v_l} = \frac{2\epsilon_r \cos \theta'_{l1}}{\epsilon_r \cos \theta'_{l1} + \sqrt{\epsilon_r - \sin^2 \theta'_{l1}}}$$

$$T_{h_l} = \frac{2 \cos \theta_{l1}}{\cos \theta_{l1} + \sqrt{\epsilon_r - \sin^2 \theta_{l1}}}$$

$$T'_{h_l} = \frac{2 \cos \theta'_{l1}}{\cos \theta'_{l1} + \sqrt{\epsilon_r - \sin^2 \theta'_{l1}}}$$

Attempts have been made to compare (4.66) with the equivalent factor resulting from the "tilted-plane" approach [5] but, unfortunately, the correspondence is not easy to establish. It appears that such a comparison might best be accomplished by comparing numerical values of (4.66) with the corresponding factor from the "tilted-plane" approach [5].

Equation (4.65) is the desired result. From this expression, one can easily obtain  $\sigma_{ab}^{\circ}$  from

$$\sigma_{ab}^{\circ} = \lim_{R \rightarrow \infty} \lim_{A \rightarrow \infty} \left\{ \frac{4\pi R^2}{A} \frac{1}{E_o^2} \left[ \langle |\delta^0 E_{ab}|^2 \rangle + \langle |\delta^1 E_{ab}|^2 \rangle \right] \right\} \quad (4.67)$$

along with the development given in [6] and as corrected in Section 2. The contribution of the zeroth order incoherent power  $\langle |\delta^0 E_{ab}|^2 \rangle$  has been previously obtained by Sancer [11] and his results can be used directly in (4.67).

### References

1. Barrick, D. E. and W. H. Peake, "A Review of Scattering from Surfaces with Different Roughness Scales," Radio Science, 3, pp. 865-68, August, 1968.
2. Wright, J. W., "A New Model for Sea Clutter," IEEE Trans. Antennas & Propagation, AP-16, pp. 217-23, March, 1968.
3. Semenov, B., "An Approximate Calculation of Scattering Of Electromagnetic Waves from a Rough Surface," Radiotekh i Elektron, (USSR), 11, pp. 1351-61, 1966.
4. Fuks, I., "Contribution to the Theory of Radio Wave Scattering on the Perturbed Sea Surface," Izv. Vyssh. Ucheb. Zaved. Radiofiz., 5, p. 876, 1966.
5. Valenzuela, G. R., M. B. Liang and J. C. Daley, "Ocean Spectra for the High Frequency Waves as Determined from Airborne Radar Measurements," J. Marine Res., 29, pp. 69-84, February, 1971.
6. Brown, G. S., "Backscattering from a Gaussian-Distributed Perfectly Conducting Rough Surface," IEEE Trans. Antennas & Propagation, AP-26, pp. 472-82, May, 1978.
7. Mitzner, K. M., "Effect of Small Irregularities on Electromagnetic Scattering From An Interface of Arbitrary Shape," J. Math. Phys., 5, pp. 1776-86, December, 1974.
8. Burrows, M. L., "A Reformulated Boundary Perturbation Theory in Electromagnetism And Its Application To A Sphere," Can. J. Phys., 45, pp. 1729-43, May, 1967.
9. Stratton, J. A., Electromagnetic Theory, McGraw-Hill Book Co., New York, see pp. 490-491, 1941.

References (Cont'd.)

10. Barrick, D. E., Radar Cross Section Handbook, Vol. 2, Ch. 9, Plenum Press, New York, 1970.
11. Sancer, M. I., "Shadow-Corrected Electromagnetic Scattering From a Randomly Rough Surface," IEEE Trans. Antennas & Propagation, AP-17, pp. 577-585, September, 1969.

## 5.0 A USEFUL RELATIONSHIP FOR THE JOINT SLOPE PROBABILITY DENSITY FUNCTION

### 5.1 Background

The incoherent power scattered in and about the specular direction depends upon the joint probability density function (jpdf) of the large scale slopes. The jpdf for the large scale slopes is also important in determining the degree of "tilt" or k-space broadening imparted to the small scale Bragg scatterers. Ideally, one would like to measure the jpdf for the large scale slopes, the roughness spectrum of the small scale heights, and the complex dielectric constant of the surface in order to predict the average scattering properties of a specified section of terrain. That is, these surface measurements would be substituted in the rough surface scattering model which, in turn, would provide an estimate of the average coherent and incoherent scattered power. From a practical point of view, measurements of the jpdf for the slopes and the small scale roughness spectrum are very difficult to obtain and the difficulty increases as the radar or electromagnetic wavelength decreases. For example, in the case of an L-band system with  $\lambda_0 = 30$  cm, the small scale part of the scattering model will require surface height spectral measurements of surface undulations having wavelengths of less than about 90 cm because  $\lambda_{\text{BRAGG}} = (\lambda_0/2)\csc\theta_1$  for backscatter. For the large scale features of the surface, the jpdf for the slopes representing surface features having spatial wavelengths greater than about 90 cm is required. Obviously, spectral information on the small scale features is going to be the most difficult to obtain. However, even the jpdf for the large scale slopes is going to be difficult to estimate. It is not unreasonable to expect that we can obtain measurements of the jpdf for the large scale heights and even the correlation function for the heights at least somewhat close to the 90 cm spatial resolution. However, this information must

somehow be translated into the jpdf for the surface slopes and this is where the difficulty comes in. We ignore the possibility of a direct measurement of the jpdf of the large scale slopes for arbitrary terrain because such a task appears to be too difficult to even contemplate.

The question basically boils down to the feasibility of translating or converting measurements of the jpdf for the surface heights into the jpdf for the surface slopes. The purpose of this section is to point out an analytical means for accomplishing this transformation and suggest that the scheme be attempted on an experimental basis. The relationship is not new and, in fact, results from some earlier rough surface scattering analysis. However, it has apparently gone unnoticed at least insofar as it applies to this very real world problem of translating the height jpdf into the slope jpdf.

## 5.2 The Transformation

Perhaps the oldest approach to estimating the quasi-specular incoherent power scattered by a rough surface is now called the autocorrelation approach. Basically, one assumes the validity of physical optics, interchanges the order of spatial integration and ensemble averaging in the expression for the scattered power, and assumes Gaussian surface statistics with the final result that the average scattered power is dependent upon the behavior of the surface height correlation function near  $|\Delta \vec{r}| = 0[1]$ . In the mid-60's, Kodis [2] showed that the average scattered power could alternatively be interpreted in terms of the number of specular points on the surface and the absolute radii of curvature at the specular points. Barrick [3] subsequently linked these two approaches in the high frequency limit where both are valid.

In the process of establishing the similarity between the autocorrelation and specular point approaches, Barrick obtained a relationship between the jpdf's of the surface heights and the surface slopes. In particular,

if  $P_{\zeta_x \zeta_y}(\zeta_x, \zeta_y)$  is the jpdf of the x and y surface slope components and  $\Phi_{\zeta_1 \zeta_2}(k_x, k_y)$  is the joint characteristic function for the surface heights  $\zeta_1(x_1, y_1)$  and  $\zeta_2(x_2, y_2)$  then [3]

$$P_{\zeta_x \zeta_y}\left(\zeta_x = -\frac{q_x}{q_z}, \zeta_y = -\frac{q_y}{q_z}\right) = \frac{q_z^2}{4\pi^2} \lim_{k_0 \rightarrow \infty} \left\{ \iint_{-\infty}^{\infty} \Phi_{\zeta_1 \zeta_2}(k_x = k_0 q_z, k_y = -k_0 q_z; \Delta x, \Delta y) \cdot \exp(j k_0 q_x \Delta x + j k_0 q_y \Delta y) d\Delta x d\Delta y \right\} \quad (5.1)$$

where  $\Delta x = x_1 - x_2$  and  $\Delta y = y_1 - y_2$ . In (5.1) the quantities  $q_x, q_y$  and  $q_z$  are limited as follows;  $|q_i| \leq 1$ ,  $i = x, y, z$ . It should be noted that both  $\Phi_{\zeta_1 \zeta_2}(\cdot)$  and  $P_{\zeta_x \zeta_y}(\cdot)$  are implicit functions of the surface height correlation function; this is how the  $(\Delta x, \Delta y)$  variation comes about in (5.1).

If an analytical form for  $\Phi_{\zeta_1 \zeta_2}$  is available then (5.1) can be used directly to obtain the jpdf for the slopes. In cases where  $\Phi_{\zeta_1 \zeta_2}(\cdot)$  is obtained from measured data, it is not immediately obvious that (5.1) is of any practical use since the behavior of the joint height characteristic function will not be known in the limit of  $k_x \rightarrow \infty$  and  $k_y \rightarrow \infty$ . However, consider the following reasoning as a means for obtaining estimates of  $P_{\zeta_x \zeta_y}(\cdot, \cdot)$ .

Since  $\Phi_{\zeta_1 \zeta_2}$  is the two-dimensional Fourier transform of the jpdf for the height, it can be obtained numerically by using a Fast Fourier Transform (FFT) on the measured jpdf height data. The result of this operation will be denoted by  $\hat{\Phi}_{\zeta_1 \zeta_2}$ . Because of measurement noise and particularly quantization noise in the measured height jpdf data,  $\hat{\Phi}_{\zeta_1 \zeta_2}$  will be limited to values less than, say,  $k_x \leq K_x$  and  $k_y \leq K_y$ . The maximum value of  $k_0$  that can be achieved in (5.1) is therefore  $\max(K_x/q_z, K_y/q_z)$ . If  $q_z$  is small then the resulting maximum value of  $k_0$  can be very large. The transform variables

in (5.1) will be given by  $K_x q_x / q_z$  and  $K_y q_y / q_z$  which may also be large, depending upon  $q_x$  and  $q_y$ . Thus, if  $q_z$  is near zero and  $\hat{P}_{\zeta_x \zeta_y}$  is computed using the following;

$$\hat{P}_{\zeta_x \zeta_y} \left( \zeta_x = -\frac{q_x}{q_z}, \zeta_y = -\frac{q_y}{q_z} \right) = \frac{q_z^2}{4\pi^2} \int_{-L}^L \int_{-L}^L \hat{\phi}_{\zeta_1 \zeta_2} (k_x = K_x, k_y = K_y; \Delta x, \Delta y) \cdot \exp \left( j \frac{K_x q_x}{q_z} \Delta x + j \frac{K_y q_y}{q_z} \Delta y \right) d\Delta x d\Delta y \quad (5.2)$$

it may turn out that  $\hat{P}_{\zeta_x \zeta_y}$  is a sufficiently good estimate of  $P_{\zeta_x \zeta_y}$  as to be useful in the scattering model. Unfortunately, this approach breaks down when  $q_x$  or  $q_y = 0$ ; however, it may be possible to get close enough to  $q_x = 0$  or  $q_y = 0$  to infer the behavior of  $P_{\zeta_x \zeta_y}$  along these lines in the  $q_x, q_y$ -plane. The limits on the integrations in (5.2) symbolically denoted as  $\pm L$ , will be determined by the correlation length of the surface, i.e. the separation distance for which the surface height correlation function is essentially zero.

An alternate approach to estimating  $P_{\zeta_x \zeta_y}$  is to examine the asymptotic behavior of  $\hat{\phi}_{\zeta_1 \zeta_2}$  as  $k_x \rightarrow K_x$  and  $k_y \rightarrow K_y$ . From this behavior, it may be possible to generate an asymptotic functional dependence of  $\hat{\phi}_{\zeta_1 \zeta_2}$  on  $k_x$  and  $k_y$ . By repeating this procedure for different values of  $\Delta x$  and  $\Delta y$ , it might be possible to also generate or build-in the functional dependence of  $\hat{\phi}_{\zeta_1 \zeta_2}$  on  $\Delta x$  and  $\Delta y$ . In this manner, the dependence of  $\hat{\phi}_{\zeta_1 \zeta_2}$  upon  $k_x, k_y, \Delta x$ , and  $\Delta y$  is obtained at least in the limit of moderately large  $k_x$  and  $k_y$ . This functional form could then be transformed according to (5.2). The major problem here is that the accuracy of the result will depend directly upon how precisely the surface height correlation function is known near  $\Delta x = 0$  and  $\Delta y = 0$ . This statement results from the fact that the behavior

of the transform of a function as  $k \rightarrow \infty$  is directly determined by the behavior of the function as  $\Delta r \rightarrow 0$  [4].

The problem of converting height jpdf data into slope jpdf results is definitely not easy. Even with the use of (5.1) the problem still poses a number of numerical complexities, primarily because of the required limit as  $k_0 \rightarrow \infty$ . However, as discussed above, (5.1) does provide some hope in solving what is otherwise a totally untractable problem. It is felt there is sufficient hope as to warrant further investigation of the utility of (5.1) in the solution of this problem.

#### References

1. Isakovich, M., "The Scattering of Waves from a Statistically Rough Surface," Zh. Eksperim. i Teor. Fiz., 23, pp. 305-14, 1952.
2. Kodis, R. D., "A Note on the Theory of Scattering from an Irregular Surface," IEEE Trans. Antennas & Propg., AP-14, pp. 77-82, January, 1966.
3. Barrick, D. E., "Relationship Between Slope Probability Density Function and the Physical Optics Integral in Rough Surface Scattering," Proc. of IEEE, 56, pp. 1728-29, October, 1968.
4. Morse, P. M. and H. Freshbach, Methods of Theoretical Physics, Vol. I, McGraw-Hill Book Company, pp. 462, 1953.



**MISSION**  
**of**  
**Rome Air Development Center**

*RADC plans and executes research, development, test and selected acquisition programs in support of Command, Control Communications and Intelligence (C<sup>3</sup>I) activities. Technical and engineering support within areas of technical competence is provided to ESD Program Offices (POs) and other ESD elements. The principal technical mission areas are communications, electromagnetic guidance and control, surveillance of ground and aerospace objects, intelligence data collection and handling, information system technology, ionospheric propagation, solid state sciences, microwave physics and electronic reliability, maintainability and compatibility.*